sciendo

CAIM
ISSN 2038-0909

Commun. Appl. Ind. Math. 10 (1), 2019, 123–152 DOI: 10.2478/caim-2019-0017

Research Article

A certified RB method for PDE-constrained parametric optimization problems

Andrea Manzoni[1*], Stefano Pagani[1]

[1]MOX - Dipartimento di Matematica, Politecnico di Milano,
Piazza Leonardo da Vinci 32, I-20133 Milano, Italy

[*]Email address for correspondence: andrea1.manzoni@polimi.it

Communicated by Giovanni Russo

Received on 06 14, 2018. Accepted on 05 17, 2019.

Abstract

We present a certified reduced basis (RB) framework for the efficient solution of PDE-constrained parametric optimization problems. We consider optimization problems (such as optimal control and optimal design) governed by elliptic PDEs and involving possibly non-convex cost functionals, assuming that the control functions are described in terms of a parameter vector. At each optimization step, the high-fidelity approximation of state and adjoint problems is replaced by a certified RB approximation, thus yielding a very efficient solution through an "optimize-then-reduce" approach. We develop a posteriori error estimates for the solutions of state and adjoint problems, the cost functional, its gradient and the optimal solution. We confirm our theoretical results in the case of optimal control/design problems dealing with potential and thermal flows.

Keywords: `PDE-constrained optimization, Reduced basis method, A posteriori error estimation, Adjoint-based approach, Non-convex cost functionals`

AMS subject classification: `49J20, 65K10, 65M15, 65M60, 65N12, 93C20`

1. Introduction

PDE-constrained optimization problems are widespread in applied sciences and engineering because of the ubiquitous need to control a system in order to reach some target. Optimal control, optimal design and (deterministic) inverse problems, can be cast within a PDE-constrained optimization framework in order to exploit a well-established theoretical setting and powerful approximation techniques [1,2]. Often, when dealing with the numerical approximation of PDE-constrained optimization problems, control variables, shapes, or unknown features to be recovered are expressed in terms of a set of parameters, featuring a much smaller dimension than the one of the discrete space used to approximate the state variable, thus recasting optimization in a more affordable low-dimensional space. Even under this assumption, numerical optimization relies on iterative procedures which usually requires a large amount of PDE solutions, evaluations of the cost functional, and possibly of its gradient with respect to control/design variables, such as in the case of descent methods or more general nonlinear programming techniques [1,2]. Obtaining a significant computational speedup within this context has been one of the leading motivations behind the development of efficient reduced order modeling techniques for PDEs in the last decade. Reduced basis (RB) methods exploiting either greedy algorithms [3–9] or proper orthogonal decomposition (POD) [10–17] have been widely applied to the solution of optimal control and shape optimization problems. More recently, conversely to the *parametric optimization problems* considered in this paper, the case of *parametrized optimal control problems* has also been addressed. In this latter case, parameters affect either differential operators or data, *but not* the control/design variables, thus characterizing multiple scenarios where an optimal control has to be determined [18–22].

In this paper we consider *PDE-constrained parametric optimization problems* ($\boldsymbol{\mu}$-OPs) where control/design variables are expressed in terms of a vector of parameters $\boldsymbol{\mu} \in \mathcal{P} \subseteq \mathbb{R}^d$, thus yielding *finite-dimensional control variables*. Parameters may affect boundary data, source terms, physical coefficients, or the geometrical configuration of the domain. Indeed, our framework is able to account for – apparently different – problems such as optimal control, parameter estimation, optimal design, which can be cast

under the form:

$$(\boldsymbol{\mu}\text{-OP}) \qquad \min_{\boldsymbol{\mu}\in\mathcal{P}_{ad}} J(\boldsymbol{\mu}) \qquad s.t. \qquad a(u(\boldsymbol{\mu}), v; \boldsymbol{\mu}) = f(v; \boldsymbol{\mu}) \qquad \forall v \in X.$$

Here $u(\boldsymbol{\mu}) \in X$ is the state solution, X is a suitable Sobolev space defined over a spatial domain $\Omega \subset \mathbb{R}^m$, $m = 1, 2, 3$, and the state constraint is given by a linear, steady, elliptic PDE (here written under weak form). Moreover, $\mathcal{P}_{ad} \subseteq \mathcal{P} \subseteq \mathbb{R}^d$, $\mathcal{P}_{ad} \neq \emptyset$, denotes a closed, convex, bounded set of admissible parameters. Furthermore, $J(\boldsymbol{\mu}) = \tilde{J}(u(\boldsymbol{\mu}), \boldsymbol{\mu})$ is a suitable cost functional, where $\tilde{J} : X \times \mathcal{P} \to \mathbb{R}$ is a quadratic function of the state u. Since the map $\boldsymbol{\mu} \mapsto u(\boldsymbol{\mu})$ is usually nonlinear, J is not a quadratic functional of $\boldsymbol{\mu}$; in general, J might not even be convex. Note that the (reduced) cost functional $J(\boldsymbol{\mu})$ is minimized with respect to $\boldsymbol{\mu}$; this latter plays here the role of optimization variable.

In several works, RB methods have been applied to parametric optimization problems just for the sake of state reduction, yielding a *reduce-then-optimize* approach; in this case, the state system is solved in a reduced state space and numerical optimization is performed according to black-box (or derivative-free) methods. In this work we rely instead on an adjoint-based approach, exploiting a RB method for the approximation of both state and adjoint problems, in order to evaluate the gradient of J in an inexpensive way during the optimization process. This can be seen as an *optimize-then-reduce* approach, that is, we first express optimality conditions as a system of (coupled) PDEs, then we construct a RB method for any $\boldsymbol{\mu}$-dependent PDE to be solved. Relying on this approach is also mandatory for deriving effective a posteriori error estimators on J, its gradient and the optimal solution.

Extending some results shown in [7,8], in this work:

1. we rely on an *adjoint-based* approach, rather than on a *sensitivity-based* approach to find the solution of the optimization problem, and compare the two options;
2. we implement a certified RB method for $\boldsymbol{\mu}$-OPs and show that the adjoint-based approach yields a stronger speedup than the sensitivity-based one;
3. we extend previous results of [7] to the case of functionals which directly depend on $\boldsymbol{\mu}$, and not only through the state solution. Moreover, compared to [7], we treat the case of quadratic functionals (with respect to the state) and set up an adjoint-based approach. Quadratic functionals were treated in the case of steady state problems in [8], however without providing a detailed error analysis, by only relying on a sensitivity-based approach. Here, we provide a detailed characterization of error estimates for the cost functional, its gradient and the optimal solution, by evaluating all the quantities appearing in their expressions in a computationally efficient way;
4. we take advantage of these error estimates to better design the optimization algorithms, in which stopping criteria are motivated by the reliability of the RB approximation, showing that both optimization and reduction stages might require a simultaneous (and careful) tuning;
5. we show that the assumption of *affine parametric dependence* required in the RB context is also crucial for the theoretical analysis of $\boldsymbol{\mu}$-OPs;
6. last, but not least, we also consider the dependence on geometrical parameters, in view of the efficient solution of optimal design problems.

Several problems which can be cast in this framework have been already tackled with reduced order modeling techniques, such as optimal control [18,23], optimal design [24–26], parameter estimation [27], model identification [28], uncertainty quantification problems [29–31]. Often this has been done neither by relying on adjoint-based approaches, nor by developing a rigorous error analysis for the optimal solution. Besides providing these two things, we assess the effect of replacing a high-fidelity approximation by a reduced-order model on the optimization process, in terms of both descent directions and optimal solutions. Hence, the numerical test cases we present deal with simple state problems, although the proposed framework can be extended to more complex applications, including also simultaneous control and design, or optimization under uncertainty [32].

The paper is organized as follows. In Sect. 2 we provide a general formulation of the class of problems we are interested in, whereas in Sect. 3 we show some well-posedness results and derive optimality

conditions (of both first and second order). We set a RB method for the solution of $\boldsymbol{\mu}$-OPs in Sect. 4, by considering either the evaluation of parametric sensitivities, or the solution of an adjoint problem. In Sect. 5 we derive a posteriori error estimates for the quantities of interest in setting the optimization procedure. Finally, we confirm our theoretical results by showing some numerical results dealing with thermal and potential flows in Sect. 6.

2. Problem setting

We deal with steady scalar problems defined over a regular and bounded domain $\Omega \subset \mathbb{R}^m$, $m = 1, 2, 3$. Let us denote by X a Sobolev space such that $H_0^1(\Omega) \subseteq X \subseteq H^1(\Omega)$, taking into account boundary conditions over $\Gamma = \partial\Omega$; X^* denotes the dual of X. The parametrized bilinear form $a(\cdot, \cdot; \boldsymbol{\mu}) : X \times X \to \mathbb{R}$ corresponds to the weak form of an elliptic, second-order parametrized differential operator; we require that, for any $\boldsymbol{\mu} \in \mathcal{P} \subset \mathbb{R}^d$, a is continuous and coercive, i.e. there exist $\alpha(\boldsymbol{\mu}) > 0$ and $M_a(\boldsymbol{\mu}) < +\infty$ such that

$$\alpha(\boldsymbol{\mu}) = \inf_{v \in X} \frac{a(v, v; \boldsymbol{\mu})}{\|v\|_X^2}, \qquad M_a(\boldsymbol{\mu}) = \sup_{u \in X} \sup_{v \in X} \frac{a(u, v; \boldsymbol{\mu})}{\|u\|_X \|v\|_X} \qquad \forall \boldsymbol{\mu} \in \mathcal{P}, \tag{1}$$

and that $f(\cdot; \boldsymbol{\mu}) \in X^*$ is continuous for any $\boldsymbol{\mu} \in \mathcal{P}$, i.e., there exist $M_f(\boldsymbol{\mu}) < +\infty$ such that

$$M_f(\boldsymbol{\mu}) = \sup_{v \in X} \frac{f(v; \boldsymbol{\mu})}{\|v\|_X} \qquad \forall \boldsymbol{\mu} \in \mathcal{P}. \tag{2}$$

In our case, parameters $\boldsymbol{\mu}$ play the role of optimization variables, that is, of *control/design* parameters. Regarding the parameter dependence in the state equation, parameters might thus affect: *(i)* the right-hand side $f(\cdot; \boldsymbol{\mu})$ if they enter into the definition of distributed and/or boundary control functions; *(ii)* the left-hand side $a(\cdot, \cdot; \boldsymbol{\mu})$, when they are related with the physical coefficients of the PDE operator; *(iii)* both a and f when they are used to parametrize the shape of the domain. When dealing with optimal design, we rely on a *fixed domain* approach, that is, the state problem originally posed on a parametrized domain $\tilde{\Omega} = \tilde{\Omega}(\boldsymbol{\mu})$ is mapped back onto a reference configuration Ω, by introducing a suitable, $\boldsymbol{\mu}$-dependent geometric map (or collection of maps) from Ω to $\tilde{\Omega}$. This is a standard procedure when dealing with RB methods [33], which also enables a strong speedup of optimal design problems by avoiding remeshing when the domain undergoes shape deformations.
Moreover, we assume that $J : \mathcal{P} \to \mathbb{R}$ is given by

$$J(\boldsymbol{\mu}) = \tilde{J}(u(\boldsymbol{\mu}), \boldsymbol{\mu}) = \frac{1}{2}\|Cu(\boldsymbol{\mu}) - z_d\|_{\mathcal{Z}}^2 + \frac{\beta}{2}\|\boldsymbol{\mu} - \boldsymbol{\mu}_d\|_{\mathbb{R}^d}^2 \tag{3}$$

being $C : X \to \mathcal{Z}$ a linear, continuous observation operator, that is, $\|Cv\|_{\mathcal{Z}} \leq \gamma \|v\|_X \ \forall v \in X$, with $\mathcal{Z}$ a suitable (Hilbert) space of observations defined over Ω. Here $z_d \in \mathcal{Z}$ is the desired target, whereas $\beta \geq 0$ and $\boldsymbol{\mu}_d \in \mathcal{P}$ is a prescribed parameter value. Here $\tilde{J}$ is a quadratic functional of the state $u(\boldsymbol{\mu})$, whereas in the more standard optimal control problems, the quadratic penalization term shall enforce the cost functional to be convex. We remark that the optimization problem above can also be meant as a parameter identification problem, aimed at finding those parameter values yielding the reference solution z_d. For the case at hand, due to the nonconvex mapping $\boldsymbol{\mu} \to u(\boldsymbol{\mu})$, the reduced cost is nonconvex, independent of the choice for $\beta \geq 0$. In particular, we consider the case $\beta = 0$ for the sake of the analysis, assuming that the solution is a strict local minimizer only for the sake of error estimation for the optimal parameters in Sect. 5.4.

Furthermore, we require the following *affine decomposition* (or parametric separability) for the forms appearing in ($\boldsymbol{\mu}$-OP), by expressing for any $\boldsymbol{\mu} \in \mathcal{P}$

$$a(u, v; \boldsymbol{\mu}) = \sum_{q=1}^{Q_a} \Theta_q^a(\boldsymbol{\mu})\ a_q(u, v), \qquad f(v; \boldsymbol{\mu}) = \sum_{q=1}^{Q_f} \Theta_q^f(\boldsymbol{\mu})\ f_q(v), \tag{4}$$

for Q_a, Q_f (real) functions $\Theta_q^a, \Theta_q^f : \mathcal{P} \to \mathbb{R}$, and (continuous) bilinear (resp. linear) forms $a_q(\cdot,\cdot) : X \times X \to \mathbb{R}$, $q = 1, \dots, Q_a$ (resp. $f_q(\cdot) : X \to \mathbb{R}$, $q = 1, \dots, Q_f$). We denote by M_a^q, $q = 1, \dots, Q_a$ (resp. M_f^q, $q = 1, \dots, Q_f$) the continuity factor of the $\boldsymbol{\mu}$-independent bilinear (resp. linear) forms.

Moreover, we express the cost functional (3) as

$$J(\boldsymbol{\mu}) = g(u(\boldsymbol{\mu}), u(\boldsymbol{\mu}); \boldsymbol{\mu}) = \sum_{q=1}^{Q_g} \Theta_q^g(\boldsymbol{\mu}) \left(\frac{1}{2} s_q(u(\boldsymbol{\mu}), u(\boldsymbol{\mu})) + l_q(u(\boldsymbol{\mu})) + C_q \right), \tag{5}$$

for Q_g functions $\Theta_q^g(\boldsymbol{\mu}) : \mathcal{P} \to \mathbb{R}$, $q = 1, \dots, Q_g$, bilinear (resp. linear) forms $s_q(\cdot,\cdot) : X \times X \to \mathbb{R}$ (resp. $l_q(\cdot) : X \to \mathbb{R}$), and scalars $C_q \in \mathbb{R}$, $q = 1, \dots, Q_g$. Here we assume that

$$(Cu(\boldsymbol{\mu}), Cu(\boldsymbol{\mu}))_{\mathcal{Z}} = \sum_{q=1}^{Q_g} \Theta_q^g(\boldsymbol{\mu}) s_q(u(\boldsymbol{\mu}), u(\boldsymbol{\mu}))$$

$$(Cu(\boldsymbol{\mu}), z_d)_{\mathcal{Z}} = \sum_{q=1}^{Q_g} \Theta_q^g(\boldsymbol{\mu}) l_q(u(\boldsymbol{\mu})), \qquad -(z_d, z_d)_{\mathcal{Z}} = \sum_{q=1}^{Q_g} \Theta_q^g(\boldsymbol{\mu}) C_q$$

because of the $\boldsymbol{\mu}$-dependence induced by the fact that the scalar product $(\cdot,\cdot)_{\mathcal{Z}}$ involves integrals over $\Omega(\boldsymbol{\mu})$. In the remainder, we consider two classes of functionals which can be cast under the form (3), by choosing either $\mathcal{Z} = H^1(\Omega_{obs})$ or $L^2(\Omega_{obs})$, C as the restriction operator over $\Omega_{obs} \subset \Omega$, a prescribed observation region, and z_d a prescribed target function.

Thus, we end up with the following formulation of problem ($\boldsymbol{\mu}$-OP):

$$\begin{aligned} &\min_{\boldsymbol{\mu} \in \mathcal{P}_{ad}} \sum_{q=1}^{Q_g} \Theta_q^g(\boldsymbol{\mu}) \left(\frac{1}{2} s_q(u(\boldsymbol{\mu}), u(\boldsymbol{\mu})) + l_q(u(\boldsymbol{\mu})) + C_q \right) \\ &\text{s.t.} \quad \sum_{q=1}^{Q_a} \Theta_q^a(\boldsymbol{\mu})\ a_q(u(\boldsymbol{\mu}), v) = \sum_{q=1}^{Q_f} \Theta_q^f(\boldsymbol{\mu})\ f_q(v) \qquad \forall v \in X. \end{aligned} \tag{6}$$

3. Well-posedness analysis and optimality conditions

Problem ($\boldsymbol{\mu}$-OP) is a special case of PDE-constrained optimization problem, where the control variable is set in a closed, bounded subset of $\mathbb{R}^d$ rather than to an infinite dimensional (Banach or Hilbert) space. Although the existence of a minimizer easily follows from Weierstrass theorem, its uniqueness is not ensured. A natural requirement for uniqueness would be the strict convexity of the cost functional with respect to the control variable $\boldsymbol{\mu}$; however, this is in general hard to satisfy, because of the nonlinear $\boldsymbol{\mu}$-dependency of the state solution, already in the simplest case of a quadratic functional of the state variable and a linear state problem. After analyzing the well-posedness of (6) and the differentiability of the state solution with respect to $\boldsymbol{\mu}$, we derive a set of first and second order optimality conditions.

3.1. *Existence of a minimizer and differentiability of the cost functional*

A further assumption concerning the map $\boldsymbol{\mu} \mapsto u(\boldsymbol{\mu})$, which also affects the cost functional, is required to show the existence of a minimizer to problem ($\boldsymbol{\mu}$-OP), as stated in the following (see the Appendix for the proof)

Proposition 3.1. *Under the following assumptions:*

1. $\mathcal{P}_{ad} \subset \mathbb{R}^d$, $\mathcal{P}_{ad} \neq \emptyset$ *is a closed, convex, and bounded set;*
2. Θ_q^a, $q = 1, \dots, Q_a$ *and* Θ_q^f, $q = 1, \dots, Q_f$ *are Lipschitz continuous functions, with constants* Λ_q^a, $\Lambda_q^f > 0$, *respectively;*
3. J *is sequentially lower continuous (with respect to* $\boldsymbol{\mu}$*),*

problem ($\boldsymbol{\mu}$-OP) admits (at least) a minimization point $(\hat{u}, \hat{\boldsymbol{\mu}}) = (u(\hat{\boldsymbol{\mu}}), \hat{\boldsymbol{\mu}})$.

Let us now investigate the differentiability of the cost functional, for which we require that the functions Θ_q^a, $q = 1, \dots, Q_a$ and Θ_q^f, $q = 1, \dots, Q_f$ are of class $C^1(\mathcal{P})$. Numerical optimization procedures such as descent methods require the evaluation of the derivatives of the cost functional $J(\boldsymbol{\mu}) = \tilde{J}(u(\boldsymbol{\mu}), \boldsymbol{\mu})$ with respect to the parameters, given by

$$\nabla_{\boldsymbol{\mu}} J(\boldsymbol{\mu}) \cdot \mathbf{e}_i = \partial_{\mu_i} J(\boldsymbol{\mu}) = \partial_u \tilde{J}\, \partial_{\mu_i} u(\boldsymbol{\mu}) + \partial_{\mu_i} \tilde{J}(\boldsymbol{\mu}). \tag{7}$$

where $\partial_u \tilde{J}$ denotes the Fréchet derivative of $\tilde{J}$ with respect to u. To ensure that J is differentiable, we must require that the map $\boldsymbol{\mu} \mapsto u(\boldsymbol{\mu})$ is differentiable, too. This property results from the *implicit function theorem*[a] (see e.g. [34]), according to the following

Proposition 3.2. *Let $A \subset X \times \mathcal{P}$ be an open subspace and $\Phi : A \to X^*$ is Fréchet differentiable, such that $\Phi(\bar{\boldsymbol{\mu}}, u(\bar{\boldsymbol{\mu}})) = 0$ and $\Phi_u(\bar{\boldsymbol{\mu}})$ is an isomorphism from X to X^*. Then, $\boldsymbol{\mu} \mapsto u(\boldsymbol{\mu})$ is a differentiable map in a neighborhood U of $\bar{\boldsymbol{\mu}}$, and $\Phi(\boldsymbol{\mu}, u(\boldsymbol{\mu})) = 0$ for any $\boldsymbol{\mu} \in U$.*

See the Appendix for the proof. By deriving (42) w.r.t. $\boldsymbol{\mu}$ we can obtain the expressions of the first-order *parametric sensitivities* of the state solution. In fact, the directional derivative $\nabla_{\boldsymbol{\mu}} u(\boldsymbol{\mu}) \cdot \boldsymbol{k}$, for any $\boldsymbol{k} \in \mathbb{R}^d$, is given by the solution of

$$a(\nabla_{\boldsymbol{\mu}} u(\boldsymbol{\mu}) \cdot \boldsymbol{k}, v; \boldsymbol{\mu}) = \sum_{q=1}^{Q_f} (\nabla_{\boldsymbol{\mu}} \Theta_q^f(\boldsymbol{\mu}) \cdot \boldsymbol{k})\ f_q(v) - \sum_{q=1}^{Q_a} (\nabla_{\boldsymbol{\mu}} \Theta_q^a(\boldsymbol{\mu}) \cdot \boldsymbol{k})\ a_q(u(\boldsymbol{\mu}), v) \quad \forall v \in X. \tag{8}$$

By choosing $\boldsymbol{k} = \mathbf{e}_i$, the i-th unit vector of the canonical basis of $\mathbb{R}^d$, (8) yields d equations for the first-order parametric sensitivities $\partial_{\mu_i} u(\boldsymbol{\mu})$, $i = 1, \dots, d$, required to express the first order optimality conditions. The derivation of these latter expressions is the goal of the following section.

3.2. *First order optimality condition*

Provided that $\mathcal{P}_{ad} \subset \mathbb{R}^d$ is a convex bounded and closed set and J is differentiable, a minimizer $\hat{\boldsymbol{\mu}}$ of (5) fulfills the following variational inequality,

$$\nabla_{\boldsymbol{\mu}} J(\hat{\boldsymbol{\mu}}) \cdot (\boldsymbol{\eta} - \hat{\boldsymbol{\mu}}) \geq 0 \qquad \forall \boldsymbol{\eta} \in \mathcal{P}_{ad}, \tag{9}$$

yielding a first-order necessary optimality condition. Therefore, we can apply the chain rule in order to evaluate

$$\nabla_{\boldsymbol{\mu}} J(\boldsymbol{\mu}) \cdot \boldsymbol{k} = \partial_u \tilde{J}(u(\boldsymbol{\mu}), \boldsymbol{\mu}) \nabla_{\boldsymbol{\mu}} u(\boldsymbol{\mu}) \cdot \boldsymbol{k} + \nabla_{\boldsymbol{\mu}} \tilde{J}(u(\boldsymbol{\mu}), \boldsymbol{\mu}) \cdot \boldsymbol{k} \qquad \forall \boldsymbol{k} \in \mathcal{P}, \tag{10}$$

where

$$\partial_u \tilde{J}(u(\boldsymbol{\mu}), \boldsymbol{\mu}) \nabla_{\boldsymbol{\mu}} u(\boldsymbol{\mu}) \cdot \boldsymbol{k} = dg(u(\boldsymbol{\mu}), \nabla_{\boldsymbol{\mu}} u(\boldsymbol{\mu}) \cdot \boldsymbol{k}; \boldsymbol{\mu})$$

and

$$\nabla_{\boldsymbol{\mu}} \tilde{J}(u(\boldsymbol{\mu}), \boldsymbol{\mu}) \cdot \boldsymbol{k} = \sum_{q=1}^{Q_g} \nabla_{\boldsymbol{\mu}} \Theta_q^g(\boldsymbol{\mu}) \cdot \boldsymbol{k}\ \left(\frac{1}{2} s_q(u(\boldsymbol{\mu}), u(\boldsymbol{\mu})) + l_q(u(\boldsymbol{\mu}) + C_q) \right). \tag{11}$$

Here, we have denoted by

$$dg(u, \psi; \boldsymbol{\mu}) = \sum_{q=1}^{Q_g} \Theta_q^g(\boldsymbol{\mu})\, (s_q(u, \psi) + l_q(\psi)) \tag{12}$$

the Fréchet derivative (with respect to u) of $g(u, u; \boldsymbol{\mu})$. In order to exploit formula (10), we need to evaluate $\nabla_{\boldsymbol{\mu}} u(\boldsymbol{\mu}) \cdot \boldsymbol{k}$ for any $\boldsymbol{k} \in \mathcal{P}$; however, sensitivities entail in principle the solution of d further parametrized PDEs (8), thus implying an extensive computational effort, although the left-hand side is still equal to the state operator.

[a] We follow this approach also in view of possible extensions to nonlinear state problems.

A more feasible approach is based on the solution of an *adjoint problem*. The adjoint approach is rather standard in PDE- constrained optimization, and requires to solve the state problem and then an auxiliary problem, depending on the derivative of the cost functional with respect to the state variable, in order to evaluate the expression of the gradient of the cost functional; see, e.g., [2] for a general introduction to this technique.

In fact, by adding (8) to (10) and choosing $v = p(\boldsymbol{\mu})$ in this latter equation, we can make the evaluation of $\nabla_{\boldsymbol{\mu}} J$ independent of $\nabla_{\boldsymbol{\mu}} u(\boldsymbol{\mu}) \cdot \boldsymbol{k}$. This goal is achieved by choosing $p = p(\boldsymbol{\mu}) \in X$ as the solution of the adjoint problem

$$\sum_{q=1}^{Q_a} \Theta_q^a(\boldsymbol{\mu}) a_q^*(p(\boldsymbol{\mu}), \psi) = \sum_{q=1}^{Q_g} \Theta_q^g(\boldsymbol{\mu}) \left\{ s_q(u(\boldsymbol{\mu}), \psi) + l_q(\psi) \right\} \qquad \forall \psi \in X \tag{13}$$

where, for any $q = 1, \ldots, Q_a$,

$$a_q^*(p, \psi) = a_q(\psi, p) \qquad \forall p, \psi \in X$$

denote q $\boldsymbol{\mu}$-independent adjoint bilinear forms. In this way, for any $\boldsymbol{k} \in \mathcal{P}$,

$$\begin{aligned} \nabla_{\boldsymbol{\mu}} J(\boldsymbol{\mu}) \cdot \boldsymbol{k} &= \nabla_{\boldsymbol{\mu}} \tilde{J}(\boldsymbol{\mu}) \cdot \boldsymbol{k} \\ &\quad - \sum_{q=1}^{Q_a} \nabla_{\boldsymbol{\mu}} \Theta_q^a(\boldsymbol{\mu}) \cdot \boldsymbol{k} \; a_q(u(\boldsymbol{\mu}), p(\boldsymbol{\mu})) + \sum_{q=1}^{Q_f} \nabla_{\boldsymbol{\mu}} \Theta_q^f(\boldsymbol{\mu}) \cdot \boldsymbol{k} \; f_q(p(\boldsymbol{\mu})). \end{aligned} \tag{14}$$

When relying on the adjoint problem, evaluating $\nabla_{\boldsymbol{\mu}} J(\boldsymbol{\mu})$ for any $\boldsymbol{k} \in \mathbb{R}^d$ requires the solution of two PDEs, in contrast to $d + 1$ PDEs which would be required when considering the solution of p sensitivity equations. This is the main reason why we consider an adjoint-based approach, instead of the sensitivity-based approach proposed e.g. in [7].

Proposition 3.3. *Let $\hat{\boldsymbol{\mu}} \in \mathcal{P}_{ad}$ be a minimizer of ($\boldsymbol{\mu}$-OP). If $\mathcal{P}_{ad} \subset \mathbb{R}^d$ is convex, bounded and closed set, there exists an adjoint state $p = p(\hat{\boldsymbol{\mu}})$ such that $(u(\hat{\boldsymbol{\mu}}), p(\hat{\boldsymbol{\mu}}), \hat{\boldsymbol{\mu}})$ satisfy the system of first-order optimality conditions:*

$$\begin{cases} \displaystyle\sum_{q=1}^{Q_a} \Theta_q^a(\hat{\boldsymbol{\mu}}) \; a_q(u(\hat{\boldsymbol{\mu}}), v) = \sum_{q=1}^{Q_f} \Theta_q^f(\hat{\boldsymbol{\mu}}) \; f_q(v) & \forall v \in X, \\ \displaystyle\sum_{q=1}^{Q_a} \Theta_q^a(\hat{\boldsymbol{\mu}}) a_q^*(p(\hat{\boldsymbol{\mu}}), \psi) = \sum_{q=1}^{Q_g} \Theta_q^g(\hat{\boldsymbol{\mu}}) \left\{ s_q(u(\boldsymbol{\mu}), \psi) + l_q(\psi) \right\} & \forall \psi \in X, \\ \nabla_{\boldsymbol{\mu}} J(\hat{\boldsymbol{\mu}}) \cdot (\boldsymbol{k} - \hat{\boldsymbol{\mu}}) \geq 0 & \forall \boldsymbol{k} \in \mathcal{P}_{ad}. \end{cases} \tag{15}$$

3.3. *Second-order optimality condition*

Provided that the functions $\Theta_q^\lambda(\cdot)$, $\lambda = a, f, g$, are of class $C^2(\mathcal{P})$, a similar adjoint-based approach can be exploited to evaluate the Hessian of the cost functional $\mathbb{H}_J(\boldsymbol{\mu}) : \mathcal{H} \to \mathbb{R}^{d \times d}$. Indeed, this latter quantity is required to implement a Newton method for numerical optimization, as well as to characterize an error estimate for the optimal parameter, see Sect. 5.4. Furthermore, a sufficient second-order condition ensuring the strict local convexity of J is the positive-definiteness of the Hessian matrix. We thus aim at evaluating the Hessian matrix $(\mathbb{H}_J(\boldsymbol{\mu}))_{ij} = \partial^2_{\mu_j \mu_i} J(\boldsymbol{\mu})$, $1 \leq i, j \leq d$ of J without relying on the second-order parametric sensitivities of the state solution, given by $(\mathbb{H}_u(\boldsymbol{\mu}))_{ij} = \partial^2_{\mu_j \mu_i} u(\boldsymbol{\mu})$, $1 \leq i, j \leq d$ – that is, by solving less then $d^2 + d + 1$ PDE problems; note that each component of $\mathbb{H}_u$ is an element of X. For the sake of simplicity, instead of the directional derivatives $\nabla_{\boldsymbol{\mu}} u(\boldsymbol{\mu}) \cdot \boldsymbol{k}$, $\nabla_{\boldsymbol{\mu}} J(\boldsymbol{\mu}) \cdot \boldsymbol{k}$, here we directly consider the partial derivatives with respect to parameter components. By taking $\boldsymbol{k} = \mathbf{e}_i$ in (11) and deriving with respect to μ_j, we get

$$(\mathbb{H}_J(\boldsymbol{\mu}))_{ij} = \partial_{\mu_j} \left(\partial_u \tilde{J}(u(\boldsymbol{\mu}), \boldsymbol{\mu}) \cdot \partial_{\mu_i} u(\boldsymbol{\mu}) \right) + \partial_{\mu_j} \left(\partial_{\mu_i} \tilde{J}(u(\boldsymbol{\mu}), \boldsymbol{\mu}) \right),$$

where

$$\partial_{\mu_j}\Big(\partial_u \tilde{J}(u(\boldsymbol{\mu}),\boldsymbol{\mu})\cdot\partial_{\mu_i}u(\boldsymbol{\mu})\Big)=\sum_{q=1}^{Q_g}\partial_{\mu_j}\Theta_q^g(\boldsymbol{\mu})\left\{s_q(u(\boldsymbol{\mu}),\partial_{\mu_i}u(\boldsymbol{\mu}))+l_q(\partial_{\mu_i}u(\boldsymbol{\mu}))\right\}$$

$$+\sum_{q=1}^{Q_g}\Theta_q^g(\boldsymbol{\mu})\left\{s_q(u(\boldsymbol{\mu}),\partial^2_{\mu_j\mu_i}u(\boldsymbol{\mu}))+l_q(\partial^2_{\mu_j\mu_i}u(\boldsymbol{\mu}))\right\} \tag{16}$$

$$+\sum_{q=1}^{Q_g}\Theta_q^g(\boldsymbol{\mu})s_q\left(\partial_{\mu_j}u(\boldsymbol{\mu}),\partial_{\mu_i}u(\boldsymbol{\mu})\right)$$

and

$$\partial_{\mu_j}\left(\partial_{\mu_i}\tilde{J}(u(\boldsymbol{\mu}),\boldsymbol{\mu})\right)=\sum_{q=1}^{Q_g}\partial^2_{\partial\mu_j\partial\mu_i}\Theta_q^g(\boldsymbol{\mu})\left\{\frac{1}{2}s_q(u(\boldsymbol{\mu}),u(\boldsymbol{\mu}))+l_q(u(\boldsymbol{\mu})+C_q)\right\}$$

$$+\sum_{q=1}^{Q_g}\partial_{\mu_i}\Theta_q^g(\boldsymbol{\mu})\left\{s_q(\partial_{\mu_j}u(\boldsymbol{\mu}),u(\boldsymbol{\mu}))+l_q(\partial_{\mu_j}u(\boldsymbol{\mu}))\right\}.$$

The second term appearing at the right-hand side of (16), namely

$$P(\boldsymbol{\mu})=\sum_{q=1}^{Q_g}\Theta_q^g(\boldsymbol{\mu})\left\{s_q(u(\boldsymbol{\mu}),\partial^2_{\mu_j\mu_i}u(\boldsymbol{\mu}))+l_q(\partial^2_{\mu_j\mu_i}u(\boldsymbol{\mu}))\right\}=dg((u(\boldsymbol{\mu}),(\mathbb{H}_u(\boldsymbol{\mu}))_{ij};\boldsymbol{\mu}), \tag{17}$$

is nothing but the right-hand side of the adjoint problem (13) where $\psi=(\mathbb{H}_u(\boldsymbol{\mu}))_{ij}$, so that

$$P(\boldsymbol{\mu})=\sum_{q=1}^{Q_a}\Theta_q^a(\boldsymbol{\mu})a_q^*(p(\boldsymbol{\mu}),(\mathbb{H}_u(\boldsymbol{\mu}))_{ij})=\sum_{q=1}^{Q_a}\Theta_q^a(\boldsymbol{\mu})a_q((\mathbb{H}_u(\boldsymbol{\mu}))_{ij},p(\boldsymbol{\mu})).$$

To avoid the evaluation of $\mathbb{H}_u(\boldsymbol{\mu})$, we can derive the state equation with respect to parameter components (similarly to what done in (8)) obtaining

$$\sum_{q=1}^{Q_a}\Theta_q^a(\boldsymbol{\mu})a_q((\mathbb{H}_u(\boldsymbol{\mu}))_{ij},v)=\sum_{q=1}^{Q_f}\partial^2_{\mu_j\mu_i}\Theta_q^f(\boldsymbol{\mu})f_q(v)-\sum_{q=1}^{Q_a}\partial^2_{\mu_j\mu_i}\Theta_q^a(\boldsymbol{\mu})\ a_q(u(\boldsymbol{\mu}),v)$$

$$-\partial_{\mu_i}a\left(\partial_{\mu_j}u(\boldsymbol{\mu}),v;\boldsymbol{\mu}\right)-\partial_{\mu_j}a\left(\partial_{\mu_i}u(\boldsymbol{\mu}),v;\boldsymbol{\mu}\right) \tag{18}$$

for any $v\in X$, where

$$\partial_{\mu_i}a\left(u,v;\boldsymbol{\mu}\right)=\sum_{q=1}^{Q_a}\partial_{\mu_i}\Theta_q^a(\boldsymbol{\mu})a_q(u,v),\qquad i=1,\dots,d. \tag{19}$$

We can thus evaluate (17) as $P(\boldsymbol{\mu})=\tilde{P}\left(u(\boldsymbol{\mu}),\partial_{\mu_1}u(\boldsymbol{\mu}),\dots,\partial_{\mu_d}u(\boldsymbol{\mu})\right)$ by taking $v=p(\boldsymbol{\mu})$ in (18). Hence, computing the Hessian matrix $\mathbb{H}_J(\boldsymbol{\mu})$ requires to evaluate only the state $u(\boldsymbol{\mu})$, the adjoint state $p(\boldsymbol{\mu})$ and the sensitivities $\partial_{\mu_i}u(\boldsymbol{\mu})$, that is, to solve $d+2$ instead of d^2+d+1 PDE problems.

4. A reduced basis method for PDE-constrained optimization

In this section we illustrate a RB method for the efficient solution of PDE-constrained parametric optimization problems under the form ($\boldsymbol{\mu}$-OP). We exploit a descent method for numerical optimization (such as the the projected gradient, Newton or quasi-Newton methods; see, e.g., [2,35]). Alternative approaches, relying, e.g., on trust region methods, have also been deeply investigated in conjunction with reduced order modeling techniques, see, e.g., [36–38]. To speedup the evaluation of the cost functional (and its gradient), which requires the solution of the state and the adjoint problems, we rely on a very cheap RB approximation of both these problems rather than on a much more expensive high-fidelity approximation.

4.1. *High-fidelity FE approximation*

Our RB method relies upon[b] a high-fidelity Finite Element (FE) approximation of the state and the adjoint problems. We introduce a FE subspace $X_h \subset X$ of dimension $N_h < +\infty$, and denote by $u_h(\boldsymbol{\mu}) \in X_h$, $p_h(\boldsymbol{\mu}) \in X_h$ the FE approximation for the state and the adjoint solution, respectively, which are obtained by solving

$$\begin{aligned} a(u_h(\boldsymbol{\mu}), v_h; \boldsymbol{\mu}) &= f(v_h; \boldsymbol{\mu}) && \forall v_h \in X_h \\ a^*(p_h(\boldsymbol{\mu}), \psi_h; \boldsymbol{\mu}) &= dg(u_h(\boldsymbol{\mu}), \psi_h; \boldsymbol{\mu})_{\mathcal{Z}} && \forall \psi_h \in X_h; \end{aligned} \tag{20}$$

here we use a more compact notation, without expliciting the affine parametric dependence. The high-fidelity approximation of problem ($\boldsymbol{\mu}$-OP) reads thus

$$\begin{aligned} &\hat{\boldsymbol{\mu}}_h = \arg\min_{\boldsymbol{\mu} \in \mathcal{P}_{ad}} J_h(\boldsymbol{\mu}) = \tilde{J}(u_h(\boldsymbol{\mu}), \boldsymbol{\mu}) \\ &\text{s.t.} \quad a(u_h(\boldsymbol{\mu}), v_h; \boldsymbol{\mu}) = f(v_h; \boldsymbol{\mu}) \qquad \forall v_h \in X_h. \end{aligned} \tag{$\boldsymbol{\mu}$-OP$_h$}$$

A descent method based on the high-fidelity approximation (20) yields a convergent sequence $\{\boldsymbol{\mu}_h^{(k)}\}_{k \geq 0} \in \mathcal{P}_{ad}$ such that

$$\boldsymbol{\mu}_h^{(k+1)} = \Pi_{\mathcal{P}_{ad}}(\boldsymbol{\mu}_h^{(k)} + \sigma_k \mathbf{d}_h^{(k)}), \qquad k = 0, 1, \dots$$

where $\Pi_{\mathcal{P}_{ad}} : \mathbb{R}^d \to \mathcal{P}_{ad}$ denotes the projection operator onto $\mathcal{P}_{ad}$ and $\mathbf{d}_h^{(k)}$ is a descent direction, such that $(\nabla_{\boldsymbol{\mu}} J(\boldsymbol{\mu}_h^{(k)}), \mathbf{d}_h^{(k)}) < 0$. Here we denote by $\nabla_{\boldsymbol{\mu}} J_h(\boldsymbol{\mu}) = \nabla_{\boldsymbol{\mu}} \tilde{J}(u_h(\boldsymbol{\mu}), \boldsymbol{\mu})$ and by $\mathbf{d}_h^{(k)}$ the descent direction, obtained e.g. as

$$\mathbf{d}_h^{(k)} = \begin{cases} -\nabla_{\boldsymbol{\mu}} J_h(\boldsymbol{\mu}_h^{(k)}) & \text{gradient method} \\ -\mathbb{H}_{\text{dfp}}^{(k)} \nabla_{\boldsymbol{\mu}} J_h(\boldsymbol{\mu}_h^{(k)}) & \text{quasi-Newton method} \\ -(\mathbb{H}_{J,h}(\boldsymbol{\mu}_h^{(k)}))^{-1} \nabla_{\boldsymbol{\mu}} J_h(\boldsymbol{\mu}_h^{(k)}) & \text{Newton method,} \end{cases} \tag{21}$$

where the step size $\sigma_k > 0$ such that $J(\boldsymbol{\mu}_h^{(k+1)}) < J(\boldsymbol{\mu}_h^{(k)})$ can be selected through an inexact line search or the so-called Armijo rule [35]. $\mathbb{H}_{\text{dfp}}^{(k)}$ is the approximation of the inverse $\mathbb{H}_{J,h}^{-1}(\boldsymbol{\mu})$ of the high-fidelity Hessian, obtained according to the iterative Davidon-Fletcher-Powell (DFP) formula:

$$\mathbb{H}_{\text{dfp}}^{(k+1)} = \mathbb{H}_{\text{dfp}}^{(k)} + \frac{(\delta\boldsymbol{\mu}_k \delta\boldsymbol{\mu}_k^T)}{\boldsymbol{y}_k^T \delta\boldsymbol{\mu}_k} - \frac{(\mathbb{H}_{\text{dfp}}^{(k)} \boldsymbol{y}_k \boldsymbol{y}_k^T \mathbb{H}_{\text{dfp}}^{(k)})}{\boldsymbol{y}_k^T \mathbb{H}_{\text{dfp}}^{(k)} \boldsymbol{y}_k}, \tag{22}$$

where $\delta\boldsymbol{\mu}_k = -\sigma_k \mathbb{H}_{\text{dfp}}^{(k)} \nabla_{\boldsymbol{\mu}} J_h(\boldsymbol{\mu}^{(k)})$ and $\boldsymbol{y}_k = \nabla_{\boldsymbol{\mu}} J_h(\boldsymbol{\mu}^{(k+1)}) - \nabla_{\boldsymbol{\mu}} J_h(\boldsymbol{\mu}^{(k)})$. Note that $\mathbb{H}_{\text{dfp}}^{(k)}$ does not require to solve problem (18) to evaluate second-order parametric sensitivities; these latter are instead required in the case of a Newton method. To ensure that the quasi-Newton update produces positive definite quasi-Newton matrices, one needs, e.g., either a Powell-Wolfe line search, or a safeguard in the update formula, by skipping the matrix update if $\boldsymbol{y}_k^T \delta\boldsymbol{\mu}_k \leq 0$. See, e.g., [39] fur further details.

Finally, given a prescribed tolerance $\varepsilon_{opt}^{tol} > 0$, we iterate until, e.g., $\|\nabla_{\boldsymbol{\mu}} J_h(\hat{\boldsymbol{\mu}}_h)\|_{\mathbb{R}^d} < \varepsilon_{opt}^{tol}$ or $\|\mathbf{d}_h\|_{\mathbb{R}^d} < \varepsilon_{opt}^{tol}$.

Remark 4.1. Due to the constrained nature of the problem, proper stopping criteria must be used to terminate the iterative methods above. For the problems we consider, the parameter space $\mathcal{P}_{ad}$ is determined by a set of inequality constraints under the form $\mu_i^{min} \leq \mu_i \leq \mu_i^{max}$, $i = 1, \dots, d$, that is, we deal with box constraints on the parameters. We also remark that, since the target z_d is generated in our setting as the state solution for a selected parameter value $\boldsymbol{\mu}_{target}$, we expect that the minima of the cost functional are internal to the parameter space, that is, all the box constraints are inactive at the minimum.

[b] The *reduction* stage does not replace the *discretization* stage of the usual *optimize-then-discretize* approach, rather it is built upon.

More rigorously, when dealing with the projected gradient method, we could use the stopping criterion based on the difference of two successive iterates, for which

$$\|\boldsymbol{\mu}_h^{(k)} - \Pi_{\mathcal{P}_{ad}}(\boldsymbol{\mu}_h^{(k)} - \sigma_k \nabla_{\boldsymbol{\mu}} J_h(\boldsymbol{\mu}_h^{(k)}))\|_{\mathbb{R}^d} < \varepsilon_{opt}^{tol}, \tag{23}$$

which indeed reduces to $\|\nabla_{\boldsymbol{\mu}} J_h(\hat{\boldsymbol{\mu}}_h)\|_{\mathbb{R}^d} < \varepsilon_{opt}^{tol}$ when the problem is unconstrained. An inexact line-search (e.g., Armijio) rule, in the case of box constraints, at each step would select the smallest $m \in \mathbb{N}$ such that, with $\eta = \beta^m$,

$$J(\Pi_{\mathcal{P}_{ad}}(\boldsymbol{\mu}_h^{(k)} + \eta \mathbf{d}_h^{(k)})) - J(\boldsymbol{\mu}_h^{(k)}) \leq -\frac{\alpha}{\eta}\|\boldsymbol{\mu}_h^{(k)} - \Pi_{\mathcal{P}_{ad}}(\boldsymbol{\mu}_h^{(k)} + \eta \mathbf{d}_h^{(k)})\|_{\mathbb{R}^d}^2$$

where typically $\beta \in [2, 10]$. A complete description of descent methods for constrained optimization problems can be found, e.g., in [39, Chapter 5].

4.2. *RB approximation*

The RB approximation of a parametrized PDE is obtained by solving a reduced problem, resulting from the (Galerkin) projection of the original problem onto a low dimensional subspace, spanned by (possibly few) snapshots of the high-fidelity problem obtained for properly selected parameter values [33]. For the case at hand, the RB approximation of the state $u_n(\boldsymbol{\mu}) \in X_n^u \subset X_h$ and the adjoint $p_n(\boldsymbol{\mu}) \in X_n^p \subset X_h$ variables solve

$$\begin{aligned} a(u_n(\boldsymbol{\mu}), v_n; \boldsymbol{\mu}) &= f(v_n; \boldsymbol{\mu}) \qquad \forall v_n \in X_n^u \\ a^*(p_n(\boldsymbol{\mu}), \psi_n; \boldsymbol{\mu}) &= dg(u_n(\boldsymbol{\mu}), \psi_n; \boldsymbol{\mu}) \; \forall \psi_n \in X_n^p. \end{aligned} \tag{24}$$

The RB approximation of problem ($\boldsymbol{\mu}$-OP$_h$) thus reads

$$\begin{aligned} &\hat{\boldsymbol{\mu}}_n = \arg\min_{\boldsymbol{\mu} \in \mathcal{P}_{ad}} J_n(\boldsymbol{\mu}) = \tilde{J}(u_n(\boldsymbol{\mu}), \boldsymbol{\mu}) \\ &\text{s.t.} \quad a(u_n(\boldsymbol{\mu}), v_n; \boldsymbol{\mu}) = f(v_n; \boldsymbol{\mu}) \qquad \forall v_n \in X_n^u. \end{aligned} \tag{$\boldsymbol{\mu}$-OP$_n$}$$

Hence, a descent method which exploits at each step the RB approximation ($\boldsymbol{\mu}$-OP$_n$) yields a convergent sequence $\{\boldsymbol{\mu}_n^{(k)}\}_{k \geq 0} \in \mathcal{P}_{ad}$ such that

$$\boldsymbol{\mu}_n^{(k+1)} = \Pi_{\mathcal{P}_{ad}}(\boldsymbol{\mu}_n^{(k)} + \sigma_k \mathbf{d}_n^{(k)}), \qquad k = 0, 1, \ldots$$

where $\mathbf{d}_n^{(k)}$ is a reduced descent direction defined as in (21)–(22) by replacing J_h with J_n; here $\nabla_{\boldsymbol{\mu}} J_n(\boldsymbol{\mu}) = \nabla_{\boldsymbol{\mu}} \tilde{J}(u_n(\boldsymbol{\mu}), \boldsymbol{\mu})$. Finally, given a a prescribed tolerance $\varepsilon_{opt}^{tol} > 0$, we iterate until, e.g., $\|\nabla_{\boldsymbol{\mu}} J_n(\hat{\boldsymbol{\mu}}_h)\|_{\mathbb{R}^d} < \varepsilon_{opt}^{tol}$ or $\|\mathbf{d}_n\|_{\mathbb{R}^d} < \varepsilon_{opt}^{tol}$. Similar considerations to the one made in Remark 4.1 also apply to the RB approximation of the optimization problem, regarding the treatment of bound constraints.

The proposed framework can also be extended to more advanced constrained optimization algorithms; our choice to adopt more straightforward descent algorithm aims at better highlighting the computational performances of the RB method when compared to the high-fidelity FE approximation.

4.3. *RB space construction*

We now address the construction of the RB spaces X_n^u, X_n^p. We exploit a greedy algorithm relying on *a posteriori* error estimates, comparing different strategies for the construction of state space and adjoint (or, alternatively, sensitivity) spaces.

First, we propose a simultaneous strategy for the state-adjoint formulation: since these two problems are not disjoint – the right-hand side of the adjoint problem depends on the state solution $u(\boldsymbol{\mu})$ – we can take advantage of the state basis when constructing the adjoint space in order to speedup the whole procedure. This yields[c] the *simultaneous state/adjoint* greedy algorithm 4.1. A second option consists in selecting the same parameter value for both state and adjoint problems at each iteration, see algorithm

[c] Indeed, in this case the adjoint solution $p_h(\mu_p^n)$ to be computed at each step depends on the state through the derivative of the cost functional with respect to the state variable; this latter problem must then be solved, additionally to the parameters μ_u^n, for each of the parameters μ_p^n.

4.2. Parameter sampling in this case is mainly driven by one of the two problems, with a consequent loss of information in the two RB spaces X_n^u, X_n^p.

The greedy algorithm can also be performed when relying on a state-sensitivity approach, instead of a state-adjoint approach. In this case, considering for instance a different sampling for each problem, we obtain algorithm 4.3. A comparison among these three algorithms is presented in Sect. 6. We denote by $Gram - Schmidt(X_n, u)$ the result of the orthonormalization of u with respect to the n elements of X_n, whereas $\Delta_n^u(\boldsymbol{\mu})$, $\Delta_n^p(\boldsymbol{\mu})$ are two error bounds for state and adjoint solutions, such that (see Sect. 5.1)

$$\|u_h(\boldsymbol{\mu}) - u_n(\boldsymbol{\mu})\|_X \leq \Delta_n^u(\boldsymbol{\mu}), \qquad \|p_h(\boldsymbol{\mu}) - p_n(\boldsymbol{\mu})\|_X \leq \Delta_n^p(\boldsymbol{\mu}) \qquad \forall \boldsymbol{\mu} \in \mathcal{P};$$

$\Delta_n^i(\boldsymbol{\mu})$, $i = 1, \dots, d$ denote instead the error bounds for the d solutions of the sensitivity equations such that, for $i = 1, \dots, d$,

$$\|\partial_{\mu_i} u_h(\boldsymbol{\mu}) - \partial_{\mu_i} u_n(\boldsymbol{\mu})\|_X \leq \Delta_n^i(\boldsymbol{\mu}) \qquad \forall \boldsymbol{\mu} \in \mathcal{P}.$$

Algorithm 4.1 Offline stage / state/adjoint, two samplings

procedure STATE-ADJOINT GREEDY ALGORITHM, TWO SAMPLINGS
Input: $n_{\max}$, ε_{RB}^{tol}, $\Xi_{train} \subset \mathcal{P}$, $\boldsymbol{\mu}_u^1, \boldsymbol{\mu}_p^1 \in \mathcal{P}$
Output: RB state and adjoint spaces X_n^u, X_n^p
  $S_n^u = \emptyset$, $X_n^u = \emptyset$, $S_n^p = \emptyset$, $X_n^p = \emptyset$
  $n = 0$, $\delta_0 = \varepsilon_{RB}^{tol} + 1$
  while $n < n_{\max}$ and $\delta_n > \varepsilon_{RB}^{tol}$ **do**
    $n \leftarrow n + 1$
    compute $u_h(\boldsymbol{\mu}_u^n)$
    $\zeta_n^u = Gram - Schmidt(X_n^u, u_h(\boldsymbol{\mu}_u^n))$
    $X_n^u \leftarrow X_n^u \cup \zeta_n^u$, $S_n^u \leftarrow S_n^u \cup \{\boldsymbol{\mu}_u^n\}$
    $[\delta_n^u, \boldsymbol{\mu}_u^n] = \arg\max_{\boldsymbol{\mu} \in \Xi_{\text{train}}} \Delta_n^u(\boldsymbol{\mu})$
    compute $p_h(\boldsymbol{\mu}_p^n)$
    $\zeta_n^p = Gram - Schmidt(X_n^p, p_h(\boldsymbol{\mu}_p^n))$
    $X_n^p \leftarrow X_n^p \cup \zeta_n^p$, $S_n^p \leftarrow S_n^p \cup \{\boldsymbol{\mu}_p^n\}$
    $[\delta_n^p, \boldsymbol{\mu}_p^n] = \arg\max_{\boldsymbol{\mu} \in \Xi_{\text{train}}} \Delta_n^p(\boldsymbol{\mu})$
    $\delta_n = \max(\delta_n^u, \delta_n^p)$

Algorithm 4.2 Offline stage / state/adjoint, one sampling

procedure STATE-ADJOINT GREEDY ALGORITHM, ONE SAMPLING
Input: $n_{\max}$, ε_{RB}^{tol}, $\Xi_{train} \subset \mathcal{P}$, $\boldsymbol{\mu}^1 \in \mathcal{P}$
Output: RB state and adjoint spaces X_n^u, X_n^p
  $S_n = \emptyset$, $X_n^u = \emptyset$,
  $n = 0$, $\delta_0 = \varepsilon_{RB}^{tol} + 1$
  while $n < n_{\max}$ and $\delta_n > \varepsilon_{RB}^{tol}$ **do**
    $n \leftarrow n + 1$
    compute $u_h(\boldsymbol{\mu}^n)$, $p_h(\boldsymbol{\mu}^n)$
    $\zeta_n^u = Gram - Schmidt(X_n^u, u_h(\boldsymbol{\mu}^n))$, $X_n^u \leftarrow X_n^u \cup \zeta_n^u$
    $\zeta_n^p = Gram - Schmidt(X_n^p, p_h(\boldsymbol{\mu}^n))$, $X_n^p \leftarrow X_n^p \cup \zeta_n^p$
    $S_n \leftarrow S_n \cup \{\boldsymbol{\mu}^n\}$
    $[\delta_n, \boldsymbol{\mu}^n] = \arg\max_{\boldsymbol{\mu} \in \Xi_{\text{train}}} (\Delta_n^u(\boldsymbol{\mu}), \Delta_n^p(\boldsymbol{\mu}))$

4.4. *Reduced optimization*

We now summarize the reduced computational procedure for the solution of a generic optimization problem through the RB method. This procedure is based on a suitable *offline-online splitting*, ensured by the affine parameter dependence assumption (4). RB spaces are thus built during a first expensive stage, performed *offline*, whereas the *online* stage consists in the optimization procedure, which requires a

Algorithm 4.3 Offline stage / sensitivities

procedure STATE-SENSITIVITIES GREEDY ALGORITHM
Input: $n_{\max}$, ε_{RB}^{tol}, $\Xi_{train} \subset \mathcal{P}$, $\boldsymbol{\mu}_u^1, \boldsymbol{\mu}_1^1, \dots, \boldsymbol{\mu}_d^1 \in \mathcal{P}$
Output: RB state and sensitivity spaces X_n^u, X_n^i, $i = 1, \dots, d$
  $S_n^u = \emptyset$, $X_n^u = \emptyset$, $S_n^i = \emptyset$, $X_n^i = \emptyset$, $i = 1, \dots, d$
  $n = 0$, $\delta_0 = \varepsilon_{RB}^{tol} + 1$
  while $n < n_{\max}$ and $\delta_n > \varepsilon_{RB}^{tol}$ **do**
    $n \leftarrow n + 1$
    compute $u_h(\boldsymbol{\mu}_u^n)$
    $\zeta_n^u = Gram - Schmidt(X_n^u, u_h(\boldsymbol{\mu}_u^n))$
    $X_n^u \leftarrow X_n^u \cup \zeta_n^u$, $S_n^u \leftarrow S_n^u \cup \{\boldsymbol{\mu}_u^n\}$
    $[\delta_n^u, \boldsymbol{\mu}_u^n] = \arg\max_{\boldsymbol{\mu} \in \Xi_{\text{train}}} \Delta_n^u(\boldsymbol{\mu})$
    for $i = 1 : d$ **do**
      compute $\partial_{\mu_k} u_h(\boldsymbol{\mu}_i^n)$
      $\zeta_n^i = Gram - Schmidt(X_n^i, \partial_{\mu_i} u_h(\boldsymbol{\mu}_i^n))$
      $X_n^i \leftarrow X_n^i \cup \zeta_n^i$, $S_n^i \leftarrow S_n^i \cup \{\boldsymbol{\mu}_i^n\}$
      $[\delta_n^i, \boldsymbol{\mu}_i^n] = \arg\max_{\boldsymbol{\mu} \in \Xi_{\text{train}}} \Delta_n^i(\boldsymbol{\mu})$
    $\delta_n = \max(\delta_n^u, \delta_n^1, \dots, \delta_n^d)$

large number of evaluations of the reduced cost functional $\tilde{J}(u_n(\boldsymbol{\mu}), \boldsymbol{\mu})$ and the reduced descent direction $\mathbf{d}_n(\boldsymbol{\mu})$. Each evaluation entails the solution of the two problems in (24), see algorithm 4.4.

The construction of the RB algebraic structures required to assemble the reduced state and adjoint problems (24) can be performed very efficiently, relying on $\boldsymbol{\mu}$-independent high-fidelity structures. The chance to assemble the high-fidelity structures by decoupling $\boldsymbol{\mu}$-dependent functions and $\boldsymbol{\mu}$-independent structures hinges upon the affine parameter dependence, and is a standard procedure in the RB context [33,40]. By relying on a RB approximation for both the state and the adjoint problems, we are able to perform efficient evaluations of the cost functional and its gradient, thus enabling to implement a reduced-order gradient or quasi-Newton method. Instead, if willing at implementing a reduced order Newton method, the RB approximation of sensitivity equations is required in order to evaluate the Hessian of the cost functional efficiently, thus implying additional costs in the *offline* procedure.

Algorithm 4.4 Online procedure

procedure REDUCED DESCENT METHOD
Input: $n_{\max}$, ε_{opt}^{tol}, $\boldsymbol{\mu}^{(0)} \in \mathcal{P}$, $\mathbf{d}_n^{(0)} \in \mathcal{P}$
Output: RB optimal solution $\hat{\boldsymbol{\mu}}_n$
  $n = 0$
  while $n < n_{\max}$ and $\|\nabla_{\boldsymbol{\mu}} J_n(\boldsymbol{\mu}_n)\| > \varepsilon_{opt}^{tol}$ **do**
    $n \leftarrow n + 1$
    compute $u_n(\boldsymbol{\mu}^{(k)})$, $p_n(\boldsymbol{\mu}^{(k)})$; evaluate $J_n(\boldsymbol{\mu}^{(k)})$, $\nabla_{\boldsymbol{\mu}} J_n(\boldsymbol{\mu}^{(k)})$
    if Gradient method **then**
      evaluate σ_k (Armijio rule / line-search)
      $\mathbf{d}_n^{(k)} = -\sigma_k \nabla_{\boldsymbol{\mu}} J_n(\boldsymbol{\mu}^{(k)})$
    if quasi-Newton method **then**
      update $H_{\text{dfp}}^{(k)}$ (DFP formula)
      $\mathbf{d}_n^{(k)} = -H_{\text{dfp}}^{(k)}(\boldsymbol{\mu}^{(k)}) \nabla_{\boldsymbol{\mu}} J_n(\boldsymbol{\mu}^{(k)})$
    if Newton method **then**
      compute $\partial_{\mu_i} u_n(\boldsymbol{\mu}^{(k)})$, $i = 1, \dots, d$ and evaluate RB Hessian $H_{J,n}(\boldsymbol{\mu}^{(k)})$
      $\mathbf{d}_n^{(k)} = -(H_{J,n}(\boldsymbol{\mu}^{(k)}))^{-1} \nabla_{\boldsymbol{\mu}} J_n(\boldsymbol{\mu}^{(k)})$
    $\boldsymbol{\mu}^{(k+1)} = \Pi_{\mathcal{P}_{ad}}(\boldsymbol{\mu}^{(k)} + \mathbf{d}_n^{(k)})$
    $k \leftarrow k + 1$
  $\hat{\boldsymbol{\mu}}_n = \boldsymbol{\mu}^{(k+1)}$

5. A posteriori error estimation

A key ingredient of the proposed framework is the capability to provide sharp error estimates for any quantity involved in the optimization process. We thus manage to keep the error between high-fidelity and reduced-order quantities under control at each optimization step, preventing the reduced optimization framework to provide inaccurate results. We highlight that evaluating efficiently a tight lower-bound $\alpha_h^{LB}(\boldsymbol{\mu}) > 0$ of the high-fidelity stability factor

$$\alpha_h(\boldsymbol{\mu}) = \inf_{v \in X} \frac{a(v, v; \boldsymbol{\mu})}{\|v\|_X^2}$$

that is, such that $\alpha_h(\boldsymbol{\mu}) \geq \alpha_h^{LB}(\boldsymbol{\mu})$ for any $\boldsymbol{\mu} \in \mathcal{P}$, plays a key role in the a posteriori error bounds; to do this, we can rely on a heuristic strategy proposed in [41] which exploits radial basis function interpolation. This latter provides an estimate $\tilde{\alpha}_h(\boldsymbol{\mu})$, rather than a lower bound $\alpha_h^{LB}(\boldsymbol{\mu})$, of the stability factor – we forgo the rigor to enhance computational efficiency. Indeed, rigorous lower bounds to the stability factor would entail a computational complexity depending inherently on $Q_a N_h^\alpha$, where the dependence on N_h is due to eigenvalues calculation (with $\alpha \in [1, 3]$). Nevertheless, $\tilde{\alpha}_h(\boldsymbol{\mu})$ provides a reliable approximation to $\alpha_h^{LB}(\boldsymbol{\mu})$, as shown in [41]. Numerical results of Sect. 6 also show that the calculated error estimates are sufficiently tight.

5.1. *State, adjoint and sensitivities approximation*

For the sake of completeness, we first report some results related with the error bound on the state and adjoint solutions, see, e.g. [33]. Let us denote by

$$\begin{aligned} r_u(v; \boldsymbol{\mu}) &= f(v; \boldsymbol{\mu}) - a(u_n(\boldsymbol{\mu}), v; \boldsymbol{\mu}) \qquad \forall v \in X_h \\ r_p(\psi; \boldsymbol{\mu}) &= dg(u_h(\boldsymbol{\mu}), \psi; \boldsymbol{\mu}) - a(\psi, p_n(\boldsymbol{\mu}); \boldsymbol{\mu}) \qquad \forall \psi \in X_h, \end{aligned} \tag{25}$$

the high-fidelity residuals for the state and the adjoint problem, evaluated over the RB solution.

Proposition 5.1. *For any $\boldsymbol{\mu} \in \mathcal{P}$, the error between the high-fidelity and the RB approximation of the state (resp. adjoint) solution is bounded by*

$$\|u_h(\boldsymbol{\mu}) - u_n(\boldsymbol{\mu})\|_X \leq \Delta_n^u(\boldsymbol{\mu}) := \frac{\|r_u(\cdot; \boldsymbol{\mu})\|_{X'}}{\alpha_h^{LB}(\boldsymbol{\mu})}, \tag{26}$$

$$\|p_h(\boldsymbol{\mu}) - p_n(\boldsymbol{\mu})\|_X \leq \frac{\|r_p(\cdot; \boldsymbol{\mu})\|_{X'}}{\alpha_h^{LB}(\boldsymbol{\mu})}. \tag{27}$$

Note that the lower bound $\alpha_h^{LB}(\boldsymbol{\mu})$ is the same in both estimates, and that the adjoint residual still depends on the high-fidelity approximation of the state variable. To overcome this issue, we can write

$$r_p(v; \boldsymbol{\mu}) = dg(u_h(\boldsymbol{\mu}), \psi; \boldsymbol{\mu}) - a(\psi, p_n(\boldsymbol{\mu}); \boldsymbol{\mu}) = r_p^n(\psi; \boldsymbol{\mu}) + dg(u_h(\boldsymbol{\mu}) - u_n(\boldsymbol{\mu}), \psi; \boldsymbol{\mu})$$

where

$$r_p^n(\psi; \boldsymbol{\mu}) = dg(u_n(\boldsymbol{\mu}), \psi; \boldsymbol{\mu}) - a(\psi, p_n(\boldsymbol{\mu}); \boldsymbol{\mu}). \tag{28}$$

The second term at the right-hand side can be easily bounded by using (26), so that a slightly alternative (but more easily computable) expression for the error bound for the adjoint solution becomes

$$\|p_h(\boldsymbol{\mu}) - p_n(\boldsymbol{\mu})\|_X \leq \Delta_n^p(\boldsymbol{\mu}) := \frac{\|r_p^n(\cdot; \boldsymbol{\mu})\|_{X'}}{\alpha_h^{LB}(\boldsymbol{\mu})} + \frac{C_{dg} \|r_u(\cdot; \boldsymbol{\mu})\|_{X'}}{(\alpha_h^{LB}(\boldsymbol{\mu}))^2}. \tag{29}$$

Here,

$$C_{dg} = \sup_{u \in X} \sup_{v \in X} \frac{dg(u, v; \boldsymbol{\mu})}{\|u\|_X \|v\|_X} < +\infty \qquad \forall \boldsymbol{\mu} \in \mathcal{P}$$

denotes the continuity constant of $dg(u,\psi;\boldsymbol{\mu})$, see equation (12).

It is indeed straightforward to obtain an error estimate for the (first-order) sensitivity equations. Subtracting the correspondent high-fidelity and reduced sensitivities (8), we obtain, for any $i=1,\dots,d$:

$$a\left(\partial_{\mu_i}u_h(\boldsymbol{\mu})-\partial_{\mu_i}u_n(\boldsymbol{\mu}),v_h;\boldsymbol{\mu}\right)=\partial_{\mu_i}a\left(u_h(\boldsymbol{\mu})-u_n(\boldsymbol{\mu}),v_h;\boldsymbol{\mu}\right)\qquad\forall v_h\in X_h.$$

Then, by using (26), the continuity and the coercivity property of $a(\cdot,\cdot;\boldsymbol{\mu})$ stated in (1), we obtain

$$\|\partial_{\mu_i}u_h(\boldsymbol{\mu})-\partial_{\mu_i}u_n(\boldsymbol{\mu})\|_X\le\Delta_n^i(\boldsymbol{\mu}):=\frac{M_{a,\mu_i}(\boldsymbol{\mu})}{\alpha_h^{LB}(\boldsymbol{\mu})}\Delta_n^u(\boldsymbol{\mu}),$$

where $M_{a,\mu_i}(\boldsymbol{\mu})$ is the continuity constant of $\partial_{\mu_i}a\left(\cdot,\cdot;\boldsymbol{\mu}\right)$, see equation (19).

5.2. *Cost functional*

We now derive an error estimate for a generic quadratic functional of $u(\boldsymbol{\mu})$ – such as the one in (3) – based on a "primal-dual" approach, inspired by the *goal-oriented* analysis of [42,43]. Being able to estimate such error is indeed crucial to ensure that the RB approximation of the cost functional – which plays the role of output of interest – is accurate enough.

Proposition 5.2. *Let $J(\boldsymbol{\mu})=g(u(\boldsymbol{\mu}),u(\boldsymbol{\mu});\boldsymbol{\mu})$ be the cost functional defined in (5), and denote by $J_h(\boldsymbol{\mu})=g(u_h(\boldsymbol{\mu}),u_h(\boldsymbol{\mu});\boldsymbol{\mu})$ and $J_n(\boldsymbol{\mu})=g(u_n(\boldsymbol{\mu}),u_n(\boldsymbol{\mu});\boldsymbol{\mu})$, respectively. Then, for any $\boldsymbol{\mu}\in\mathcal{P}$,*

$$|J_h(\boldsymbol{\mu})-J_n(\boldsymbol{\mu})|\le\Delta_n^J(\boldsymbol{\mu}):=\frac{\|r_u(\cdot;\boldsymbol{\mu})\|_{X'}\|r_p^n(\cdot;\boldsymbol{\mu})\|_{X'}}{\alpha_h^{LB}(\boldsymbol{\mu})}+C_{dg}\frac{\|r_u(\cdot;\boldsymbol{\mu})\|_{X'}^2}{(\alpha_h^{LB}(\boldsymbol{\mu}))^2}.\tag{30}$$

Proof. We rely on the introduction of a Lagrangian functional

$$\mathcal{L}(u,p;\boldsymbol{\mu})=J(\boldsymbol{\mu})+f(p;\boldsymbol{\mu})-a(u,p;\boldsymbol{\mu})$$

in order to rewrite the difference $|J_h(\boldsymbol{\mu})-J_n(\boldsymbol{\mu})|$ by combining in an appropriate manner the state and the adjoint problems, as well as their residuals. Note that all the derivation is carried out at a fixed value of $\boldsymbol{\mu}$. Denoting by

$$\begin{aligned}\mathcal{L}(u_h,p_h;\boldsymbol{\mu})&=J_h(\boldsymbol{\mu})-a(u_h,p_h;\boldsymbol{\mu})+f(p_h;\boldsymbol{\mu}),\\ \mathcal{L}(u_n,p_n;\boldsymbol{\mu})&=J_n(\boldsymbol{\mu})-a(u_n,p_n;\boldsymbol{\mu})+f(p_n;\boldsymbol{\mu})\end{aligned}$$

we obtain that $J_h(\boldsymbol{\mu})-J_n(\boldsymbol{\mu})=\mathcal{L}(u_h,p_h;\boldsymbol{\mu})-\mathcal{L}(u_n,p_n;\boldsymbol{\mu})$. For the sake of notation, we denote by $\mathbf{x}_h=(u_h,p_h)$, $\mathbf{x}_n=(u_n,p_n)$ and $\mathbf{e}_h=(u_h-u_n,p_h-p_n)$; $\boldsymbol{\mu}$-dependence is understood. Note that, by definition of $\mathcal{L}(\cdot,\cdot;\boldsymbol{\mu})$, for all $\mathbf{y}_h=(v_h,q_h)\in X_h$

$$\begin{aligned}\mathcal{L}'(\mathbf{x}_h;\mathbf{y}_h;\boldsymbol{\mu})&:=\mathcal{L}'_u((u_h,p_h);v_h;\boldsymbol{\mu})+\mathcal{L}'_p((u_h,p_h);q_h;\boldsymbol{\mu})\\ &=[dg(u_h(\boldsymbol{\mu}),v_h;\boldsymbol{\mu})-a(v_h,p_h(\boldsymbol{\mu});\boldsymbol{\mu})]+[f(q_h;\boldsymbol{\mu})-a(u_h(\boldsymbol{\mu}),q_h;\boldsymbol{\mu})]=0.\end{aligned}\tag{31}$$

Hence, we have

$$\begin{aligned}J_h(\boldsymbol{\mu})-J_n(\boldsymbol{\mu})=\mathcal{L}(\mathbf{x}_h;\boldsymbol{\mu})-\mathcal{L}(\mathbf{x}_n;\boldsymbol{\mu})&=\int_0^1\mathcal{L}'(\mathbf{x}_n+s\mathbf{e}_h;\mathbf{e}_h;\boldsymbol{\mu})ds\\ &+\frac{1}{2}\mathcal{L}'(\mathbf{x}_n;\mathbf{e}_h;\boldsymbol{\mu})-\frac{1}{2}\mathcal{L}'(\mathbf{x}_n;\mathbf{e}_h;\boldsymbol{\mu})-\frac{1}{2}\mathcal{L}'(\mathbf{x}_h;\mathbf{e}_h;\boldsymbol{\mu});\end{aligned}$$

note that $\mathcal{L}'(\mathbf{x}_h;\mathbf{e}_h;\boldsymbol{\mu})=0$ thanks to (31). The last two terms on the right hand side are just the approximation of the second one by the trapezoidal rule. Therefore,

$$J_h(\boldsymbol{\mu})-J_n(\boldsymbol{\mu})=\frac{1}{2}\mathcal{L}'(\mathbf{x}_n;\mathbf{e}_h;\boldsymbol{\mu})+R$$

where the remainder term of the trapezoidal rule is

$$R=\frac{1}{2}\int_0^1\mathcal{L}'''(\mathbf{x}_n+s\mathbf{e}_h;\mathbf{e}_h,\mathbf{e}_h,\mathbf{e}_h;\boldsymbol{\mu})ds$$

and it vanishes because of the linearity of $a(\cdot,\cdot;\boldsymbol{\mu})$ and of $f(\cdot;\boldsymbol{\mu})$. Since

$$\mathcal{L}'(\mathbf{x}_n;\mathbf{e}_h;\boldsymbol{\mu}) = r_p^n(u_h(\boldsymbol{\mu})-u_n(\boldsymbol{\mu});\boldsymbol{\mu}) + r_u(p_h(\boldsymbol{\mu})-p_n(\boldsymbol{\mu});\boldsymbol{\mu})$$

according to (25) and to (28), we find that

$$|J_h(\boldsymbol{\mu})-J_n(\boldsymbol{\mu})| \le \frac{1}{2}\|r_u\|_{X'}\|p_h(\boldsymbol{\mu})-p_n(\boldsymbol{\mu})\|_X + \frac{1}{2}\|r_p^n\|_{X'}\|u_h(\boldsymbol{\mu})-u_n(\boldsymbol{\mu})\|_X,$$

thanks to Cauchy-Schwarz inequality; estimate (30) finally follows by (26) and (29). □

5.3. *Gradient of the cost functional*

Being able to estimate the error on the gradient of the cost functional ensures that the descent directions $\mathbf{d}_n^{(k)}$ of the reduced minimization algorithm are indeed very close to the directions $\mathbf{d}_h^{(k)}$ we would have built by considering the high-fidelity approximation. Estimating the error $\|\nabla_{\boldsymbol{\mu}} J_h(\boldsymbol{\mu}) - \nabla_{\boldsymbol{\mu}} J_n(\boldsymbol{\mu})\|_{\mathbb{R}^d}$ is usually quite involved and results in not so tight error bounds.

In this work we take advantage of the primal-dual approach in order to improve this estimate. For any $i=1,\dots,d$, let us denote by

$$\partial_{\mu_i} f(v;\boldsymbol{\mu}) = \sum_{q=1}^{Q_f} \partial_{\mu_i}\Theta_q^f(\boldsymbol{\mu}) f_q(v), \tag{32}$$

$$\partial_{\mu_i} s(u,v;\boldsymbol{\mu}) = \sum_{q=1}^{Q_g} \partial_{\mu_i}\Theta_q^g(\boldsymbol{\mu}) s_q(u,v), \quad \partial_{\mu_i} l(v;\boldsymbol{\mu}) = \sum_{q=1}^{Q_g} \partial_{\mu_i}\Theta_q^g(\boldsymbol{\mu}) l_q(v), \tag{33}$$

and by $M_{f,\mu_i}(\boldsymbol{\mu})$, $M_{s,\mu_i}(\boldsymbol{\mu})$, $M_{l,\mu_i}(\boldsymbol{\mu})$ the continuity constants of the forms defined in (32)–(33).

Proposition 5.3. *Under the assumptions of Proposition 5.2, for any* $\boldsymbol{\mu}\in\mathcal{P}$

$$\|\nabla_{\boldsymbol{\mu}} J_h(\boldsymbol{\mu}) - \nabla_{\boldsymbol{\mu}} J_n(\boldsymbol{\mu})\|_{\mathbb{R}^d} \le \Delta_n^{\nabla J}(\boldsymbol{\mu}) := \left(\sum_{i=1}^d \left(C_i^u(\boldsymbol{\mu})\Delta_n^u(\boldsymbol{\mu}) + C_i^p(\boldsymbol{\mu})\Delta_n^p(\boldsymbol{\mu})\right)^2\right)^{1/2} \tag{34}$$

where

$$C_i^u(\boldsymbol{\mu}) = M_a(\boldsymbol{\mu})\|p_n(\boldsymbol{\mu})\|_X \frac{M_{a,\mu_i}(\boldsymbol{\mu})}{\alpha_h^{LB}(\boldsymbol{\mu})} + \left(2M_{s,\mu_i}\frac{M_f(\boldsymbol{\mu})}{\alpha_h^{LB}(\boldsymbol{\mu})} + M_{l,\mu_i}(\boldsymbol{\mu})\right),$$
$$C_i^p(\boldsymbol{\mu}) = M_{f,\mu_i}(\boldsymbol{\mu}) + M_{a,\mu_i}(\boldsymbol{\mu})\frac{M_f(\boldsymbol{\mu})}{\alpha_h^{LB}(\boldsymbol{\mu})}.$$

Proof. For each component μ_i, $i=1,\dots,d$, using the chain rule (7) and the adjoint problem (13) we obtain

$$\begin{aligned}|D_{\mu_i}J_h - D_{\mu_i}J_n| &\le |\partial_{u_h}J_h\partial_{\mu_i}u_h(\boldsymbol{\mu}) - \partial_{u_n}J_n\partial_{\mu_i}u_n(\boldsymbol{\mu})| + |\partial_{\mu_i}J_h - \partial_{\mu_i}J_n| \\ &= |a^*(p_h(\boldsymbol{\mu}),\partial_{\mu_i}u_h(\boldsymbol{\mu});\boldsymbol{\mu}) - a^*(p_n(\boldsymbol{\mu}),\partial_{\mu_i}u_n(\boldsymbol{\mu});\boldsymbol{\mu})| + |\partial_{\mu_i}J_h - \partial_{\mu_i}J_n| = I + II\end{aligned}$$

We proceed separately for the two terms. For the former, we add and subtract $a(p_n(\boldsymbol{\mu}),\partial u_h(\boldsymbol{\mu})/\partial\mu_i;\boldsymbol{\mu})$ and apply Cauchy-Schwarz inequality, obtaining

$$I \le |a^*(p_h(\boldsymbol{\mu})-p_n(\boldsymbol{\mu}),\partial_{\mu_i}u_h(\boldsymbol{\mu});\boldsymbol{\mu})| + |a^*(p_n(\boldsymbol{\mu}),\partial_{\mu_i}u_h(\boldsymbol{\mu})-\partial_{\mu_i}u_n(\boldsymbol{\mu});\boldsymbol{\mu})| = I_a + I_b.$$

We estimate I_b using the continuity of $a^*(\cdot,\cdot;\boldsymbol{\mu})$, that is,

$$I_b \le M_a(\boldsymbol{\mu})\|p_n(\boldsymbol{\mu})\|_X\,|\partial_{\mu_i}u_h(\boldsymbol{\mu})-\partial_{\mu_i}u_n(\boldsymbol{\mu})|_X \le M_a(\boldsymbol{\mu})\|p_n(\boldsymbol{\mu})\|_X\frac{M_{a,\mu_i}(\boldsymbol{\mu})}{\alpha_h^{LB}(\boldsymbol{\mu})}\Delta_n^u(\boldsymbol{\mu});$$

while, using the problem for the (first-order) sensitivity, we obtain

$$\begin{aligned} I_a &= |a\left(\partial_{\mu_i} u_h(\boldsymbol{\mu}), p_h(\boldsymbol{\mu}) - p_n(\boldsymbol{\mu}); \boldsymbol{\mu}\right)| = |\partial_{\mu_i} f(p_h(\boldsymbol{\mu}) - p_n(\boldsymbol{\mu})) - \partial_{\mu_i} a\left(u_h(\boldsymbol{\mu}), p_h(\boldsymbol{\mu}) - p_n(\boldsymbol{\mu}); \boldsymbol{\mu}\right)| \\ &\leq M_{f,\mu_i}(\boldsymbol{\mu}) \|p_h(\boldsymbol{\mu}) - p_n(\boldsymbol{\mu})\|_X + M_{a,\mu_i}(\boldsymbol{\mu}) \frac{M_f(\boldsymbol{\mu})}{\alpha_h^{LB}(\boldsymbol{\mu})} \|p_h(\boldsymbol{\mu}) - p_n(\boldsymbol{\mu})\|_X \\ &\leq \left(M_{f,\mu_i}(\boldsymbol{\mu}) + M_{a,\mu_i}(\boldsymbol{\mu}) \frac{M_f(\boldsymbol{\mu})}{\alpha_h^{LB}(\boldsymbol{\mu})} \right) \Delta_n^p(\boldsymbol{\mu}). \end{aligned}$$

For the latter, using the continuity of the forms defined in (33), we obtain

$$\begin{aligned} II &= |\partial_{\mu_i} s(u_h(\boldsymbol{\mu}), u_h(\boldsymbol{\mu}); \boldsymbol{\mu}) + \partial_{\mu_i} l(u_h(\boldsymbol{\mu})) - \partial_{\mu_i} s(u_n(\boldsymbol{\mu}), u_n(\boldsymbol{\mu})) - \partial_{\mu_i} l(u_n(\boldsymbol{\mu}))| \\ &\leq M_{s,\mu_i}(\|u_h(\boldsymbol{\mu})\|_X + \|u_n(\boldsymbol{\mu})\|_X)\|u_h(\boldsymbol{\mu}) - u_n(\boldsymbol{\mu})\|_X + M_{l,\mu_i}\|u_h(\boldsymbol{\mu}) - u_n(\boldsymbol{\mu})\| \\ &\leq \left(2M_{s,\mu_i}(\boldsymbol{\mu}) \frac{M_f(\boldsymbol{\mu})}{\alpha_h^{LB}(\boldsymbol{\mu})} + M_{l,\mu_i}(\boldsymbol{\mu}) \right) \Delta_n^u(\boldsymbol{\mu}). \end{aligned}$$

By combining the previous inequalities, (34) follows. □

5.4. *Optimal solution*

The minimizer of $J_n(\boldsymbol{\mu})$ is a suboptimal solution of the optimization problem; it is then crucial to be able to estimate the error $\|\hat{\boldsymbol{\mu}}_h - \hat{\boldsymbol{\mu}}_n\|_{\mathbb{R}^d}$ between the *true* minimum – that is, the one we would obtain by minimizing $J_h(\boldsymbol{\mu})$ – and $\hat{\boldsymbol{\mu}}_n$, the solution of the reduced optimization problem, in order to assess the reliability of this latter. In the case both $\hat{\boldsymbol{\mu}}_h$ and $\hat{\boldsymbol{\mu}}_n$ are strict local minima[d] of problem ($\boldsymbol{\mu}$-OP$_h$) and ($\boldsymbol{\mu}$-OP$_n$), respectively, it is possible to provide an estimate for the error $\|\hat{\boldsymbol{\mu}}_h - \hat{\boldsymbol{\mu}}_n\|_{\mathbb{R}^d}$, by combining the previous results. This ensures that the reduced optimization method converges to an optimal solution $\hat{\boldsymbol{\mu}}_n$ which is close to the high-fidelity solution $\hat{\boldsymbol{\mu}}_h$ up to a prescribed threshold.

Let us then assume that $\boldsymbol{\mu}_h \in \mathcal{P}$ is such that $\nabla_{\boldsymbol{\mu}} J_h(\hat{\boldsymbol{\mu}}_h) = \mathbf{0}$, and denote by $\mathbb{H}_{J,h}(\boldsymbol{\mu})$ the *high-fidelity* Hessian of the cost functional (see Sect. 3.3). Moreover, let $\hat{\boldsymbol{\mu}}_n \in \mathcal{P}$ be the approximate solution to problem ($\boldsymbol{\mu}$-OP$_n$) fulfilling, for some $\epsilon_J > 0$,

$$\|\nabla_{\boldsymbol{\mu}} J_n(\hat{\boldsymbol{\mu}}_n)\|_{\mathbb{R}^d} \leq \epsilon_J;$$

as already pointed out in Remark 4.1, a more appropriate stopping criterion is provided by (23). However, here we assume that the solution of the optimization problem is a strict local minimizer – this is also justified by the particular choice of the target z_d we made. We also denote by $\bar{B}_r(\boldsymbol{\mu})$ a closed ball with center $\boldsymbol{\mu} \in \mathcal{P}$ and radius $r > 0$. Then, the following error estimate holds for optimal parameters.

Theorem 5.1. *Denote by*

$$\lambda = \|\mathbb{H}_{J,h}(\hat{\boldsymbol{\mu}}_n)^{-1}\|_{\mathbb{R}^{d\times d}}, \qquad \epsilon = \|\nabla_{\boldsymbol{\mu}} J_h(\hat{\boldsymbol{\mu}}_n) - \nabla_{\boldsymbol{\mu}} J_n(\hat{\boldsymbol{\mu}}_n)\|_{\mathbb{R}^d} + \epsilon_J.$$

and by $L(r) = \sup_{\boldsymbol{\mu}\in\bar{B}_r(\hat{\boldsymbol{\mu}}_n)} \|\mathbb{H}_{J,h}(\hat{\boldsymbol{\mu}}_n) - \mathbb{H}_{J,h}(\boldsymbol{\mu}))\|_{\mathbb{R}^{d\times d}}$. *Provided that*

$$2\lambda \cdot L(2\lambda\epsilon) \leq 1 \tag{35}$$

there exists a unique solution $\hat{\boldsymbol{\mu}}_h \in \bar{B}_{2\lambda\epsilon}(\hat{\boldsymbol{\mu}}_n)$ *of the optimization problem* ($\boldsymbol{\mu}$-OP$_h$), *such that*

$$\|\hat{\boldsymbol{\mu}}_h - \hat{\boldsymbol{\mu}}_n\| \leq 2\lambda\epsilon. \tag{36}$$

[d] This result essentially allows to build an approximation to the nonlinear equation $\nabla_{\boldsymbol{\mu}} J_h(\hat{\boldsymbol{\mu}}_h) = \mathbf{0}$, that is, requires the minimizer $\hat{\boldsymbol{\mu}}_h$ (as well as $\hat{\boldsymbol{\mu}}_n$) to be a strict local minimum for an unconstrained optimization problem. The optimization problem at hand is necessarily defined on a bounded and convex set (since $\mathcal{P}_{ad} \subseteq \mathcal{P}$, where $\mathcal{P} \subset \mathbb{R}^d$ is the parameter space in which the training of the RB approximation is conducted). Only for the sake of error estimation on the optimal parameter, a possible way to make the problem at hand *unconstrained* is to set $J(\boldsymbol{\mu}) = K$ for $\boldsymbol{\mu} \notin \mathcal{P}$ with $K \gg 1$. Note that for the cases at hand, one can expect that minimizers are interior points to $\mathcal{P}_{ad}$, since the target z_d corresponds to a given parameter instance.

Proof. We do not report the full proof for the sake of space; the interested reader can refer, e.g., to [44,45]. It is straightforward to see that the solution $\hat{\boldsymbol{\mu}}_h$ to problem ($\boldsymbol{\mu}$-OP$_h$) is a fixed point of the map $\boldsymbol{\Phi} : \mathbb{R}^d \to \mathbb{R}^d$ defined by $\boldsymbol{\Phi}(\boldsymbol{\mu}) = \boldsymbol{\mu} - \mathbb{H}_{J,h}(\hat{\boldsymbol{\mu}}_n)^{-1} \nabla_{\boldsymbol{\mu}} J_h(\boldsymbol{\mu})$, since $\nabla_{\boldsymbol{\mu}} J_h(\hat{\boldsymbol{\mu}}_h) = \mathbf{0}$. The general Brezzi-Rappaz-Raviart theory (see, e.g. [45, Section 2] provides existence and uniqueness of the fixed point, as well as the error bound (36). □

Similarly to previous bounds, the error bound (36) combines two terms: λ, which plays the role of a stability factor, and ε, which can be considered as the dual norm of the residual of the minimization problem $\nabla_{\boldsymbol{\mu}} J_h(\boldsymbol{\mu}) = \mathbf{0}$. Evaluating the (inverse norm of the) high-fidelity Hessian $\mathbb{H}_{J,h}(\cdot)$ entails the solution of the high-fidelity state (and adjoint) problem for $\boldsymbol{\mu} = \hat{\boldsymbol{\mu}}_n$; however, this computation has to be performed only when reaching the stopping criterion on the reduced optimization, if we want to certify the optimal solution through a bound of the error $\|\hat{\boldsymbol{\mu}}_h - \hat{\boldsymbol{\mu}}_n\|_{\mathbb{R}^d}$. A possible alternative when multiple evaluations of the error bound (36) are required would be to rely on interpolation procedures (in the parameter space), similarly to what done for the approximation of stability factors [41].

Remark 5.1. By combining error estimates (30), (34) and (36), we can also provide an indication on the error between the values of the cost functionals evaluated at the minimization points. Indeed, since

$$J_h(\hat{\boldsymbol{\mu}}_h) - J_n(\hat{\boldsymbol{\mu}}_n) = (J_h(\hat{\boldsymbol{\mu}}_h) - J_n(\hat{\boldsymbol{\mu}}_h)) \; + \; (J_n(\hat{\boldsymbol{\mu}}_h) - J_n(\hat{\boldsymbol{\mu}}_n))$$

by considering the Taylor expansion of $J_n(\hat{\boldsymbol{\mu}}_h) - J_n(\hat{\boldsymbol{\mu}}_n) \approx \nabla_{\boldsymbol{\mu}} J_n(\hat{\boldsymbol{\mu}}_n) \cdot (\hat{\boldsymbol{\mu}}_h - \hat{\boldsymbol{\mu}}_n)$ at $\hat{\boldsymbol{\mu}}_n$, and neglecting terms of order higher than one provided $\hat{\boldsymbol{\mu}}_h - \hat{\boldsymbol{\mu}}_n$ is sufficiently small, we obtain

$$|J_h(\hat{\boldsymbol{\mu}}_h) - J_n(\hat{\boldsymbol{\mu}}_n)| \lesssim \Delta_n^J(\hat{\boldsymbol{\mu}}_h) + \epsilon_J \cdot 2\lambda\epsilon.$$

While the latter term appearing at the right-hand side is computable, the former is not; however, by assuming that $\Delta_n^J(\hat{\boldsymbol{\mu}}_h) \approx \Delta_n^J(\hat{\boldsymbol{\mu}}_n)$ provided that $\hat{\boldsymbol{\mu}}_h - \hat{\boldsymbol{\mu}}_n$ is sufficiently small, we can estimate the error on the cost functionals evaluated at the minimization points as $|J_h(\hat{\boldsymbol{\mu}}_h) - J_n(\hat{\boldsymbol{\mu}}_n)| \lesssim \Delta_n^J(\hat{\boldsymbol{\mu}}_n) + \epsilon_J \cdot 2\lambda\epsilon$.

In the following section we show the effectivity of the proposed error estimates, and we assess the computational performances of our reduced optimization framework.

6. Numerical results

In this section we present some numerical results dealing with quadratic cost functional and elliptic scalar stationary PDE, characterized by physical and/or geometric parameters playing the role of control variables[e]. Simple physical problems have been chosen to better highlight properties and performances of the proposed computational strategies. After performing the offline stage, the inexpensive RB online evaluation takes place at each iteration of the optimization scheme. Although in our results the target z_d is fixed, we highlight that the proposed framework can also be used to solve optimization problems for different target functions z_d (possibly depending on $\boldsymbol{\mu} \in \mathcal{P}$) without requiring a new offline stage.

6.1. *Graetz conduction-convection problem*

The Graetz problem concerns the forced convection of a heat flow in a pipeline with walls at variable temperature. We deal with a parametrized version of this problem, where $d = 4$ parameters are:

- $\mu_1 \in [1, 5]$ the length of the pipe section;
- $\mu_2 \in [1, 7]$, being μ_2^2 the Péclet number;
- $\mu_3 \in [0, \frac{\pi}{4}]$ the angle of incidence of the advection field;
- $\mu_4 \in [0, \frac{\pi}{2}]$ the amplitude of the inlet Dirichlet boundary condition.

[e] Computations have been run on a laptop with a 2,2 GHz Intel Core i7 processor and 8 GB of RAM.

We consider the domain $\tilde{\Omega}(\boldsymbol{\mu}) = (0, 3+\mu_1) \times (0,1)$; in the first subregion $(0, 1+\mu_1) \times (0,1)$ the flow comes in contact with the hot wall $\Gamma_{in} = \Gamma_{in}^1 \cup \Gamma_{in}^2$, whereas in the second (observation) region $(1+\mu_1, 3+\mu_1) \times (0,1)$ the fluid flows through cold walls. The state problem (for the temperature variable) reads as follows: find $u(\boldsymbol{\mu})$ such that

$$
\begin{cases}
-\dfrac{1}{\mu_2^2}\Delta u(\boldsymbol{\mu}) + \mathbf{b}(\mu_3)\cdot\nabla u(\boldsymbol{\mu}) = 0 & \text{in } \tilde{\Omega}(\mu_1) \\
u(\boldsymbol{\mu}) = 0 & \text{on } \tilde{\Gamma}_D \\
u(\boldsymbol{\mu}) = \cos(\mu_4)(1-x_1)(x_1-1-\mu_1) & \text{on } \tilde{\Gamma}_{in}^1(\mu_1) \\
u(\boldsymbol{\mu}) = \sin(\mu_4)(1-x_1)(x_1-1-\mu_1) & \text{on } \tilde{\Gamma}_{in}^2(\mu_1) \\
\dfrac{\partial u(\boldsymbol{\mu})}{\partial \mathbf{n}} = 0 & \text{on } \tilde{\Gamma}_{out},
\end{cases} \tag{37}
$$

where $\mathbf{b}(\mu_3) = [\cos(\mu_3)10x_2(1-x_2), -\sin(\mu_3)]$. Given a target z_d, the goal is to approximate, through the reduced framework, the solution

$$
\hat{\boldsymbol{\mu}}_h = \arg\min_{\boldsymbol{\mu}\in\mathcal{P}} J_h(\boldsymbol{\mu}), \quad J_h(\boldsymbol{\mu}) = \frac{1}{2}\|u_h(\boldsymbol{\mu}) - z_d\|^2_{L^2(\tilde{\Omega}_{obs}(\boldsymbol{\mu}))}, \tag{38}
$$

the minimum of J_h being reached for $\hat{\boldsymbol{\mu}} = \boldsymbol{\mu}_{target}$, i.e. $J_h(\hat{\boldsymbol{\mu}}) = 0$. For the sake of numerical test, we set $\boldsymbol{\mu}_{target} = [3, 4, \frac{\pi}{10}, 1]$ and the corresponding high-fidelity solution $u_h(\boldsymbol{\mu}_{target})$ as target z_d.

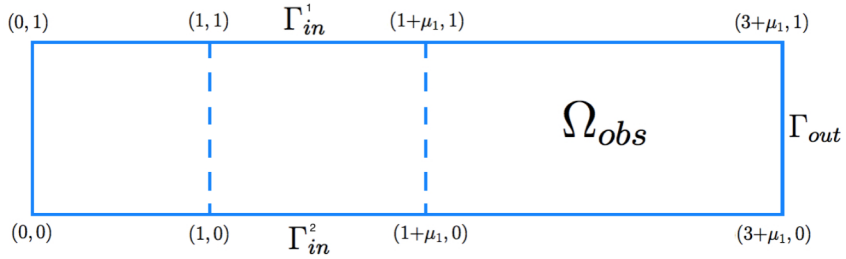

Figure 1. Schematic representation of the domain $\Omega(\boldsymbol{\mu})$ relative to the Graetz problem (37).

6.1.1. *Offline stage*

After mapping the problem (37)-(38) onto a fixed reference domain Ω, we construct a high-fidelity approximation through the Galerkin FE method, using piecewise linear elements; the dimension of the corresponding space is $N_h = 4033$. The affine parametric dependence (4) is recovered through $Q_a = 7$ and $Q_f = 15$ terms, respectively. Then, we turn to the construction of a RB approximation for both the state and the adjoint problem.

For the sake of comparison, we consider the three greedy algorithms introduced in Sect. 4.3. Numerical results presented in Fig. 2 outline two main evidences: the adjoint-based approach enables to obtain a RB space of lower dimension keeping the same accuracy level with respect to the sensitivity-based approach (see Fig. 2, left). Moreover (see Fig. 2, right), the adjoint-based approach performs better when the snapshots for the state and the adjoint problems are computed with respect to parameter values independently sampled (Algorithm 4.1, two samplings) – that is, the retained parameter sets S_n^u and S_n^p are different (see Fig. 3). For this reason, we consider only Algorithms 4.1 and 4.3 for the sake of comparison.

The three proposed strategies show different *offline* computational costs: indeed, the need of constructng a RB space for each of the $d > 1$ sensitivity equations has a considerable impact, which becomes larger and larger as the RB space dimension N increases; see Table 6.1.1.

The adjoint-based strategy relying on two independent sampling for the construction of state and adjoint subspaces (Algorithm 4.1) is the best approach in terms of both efficiency and accuracy.

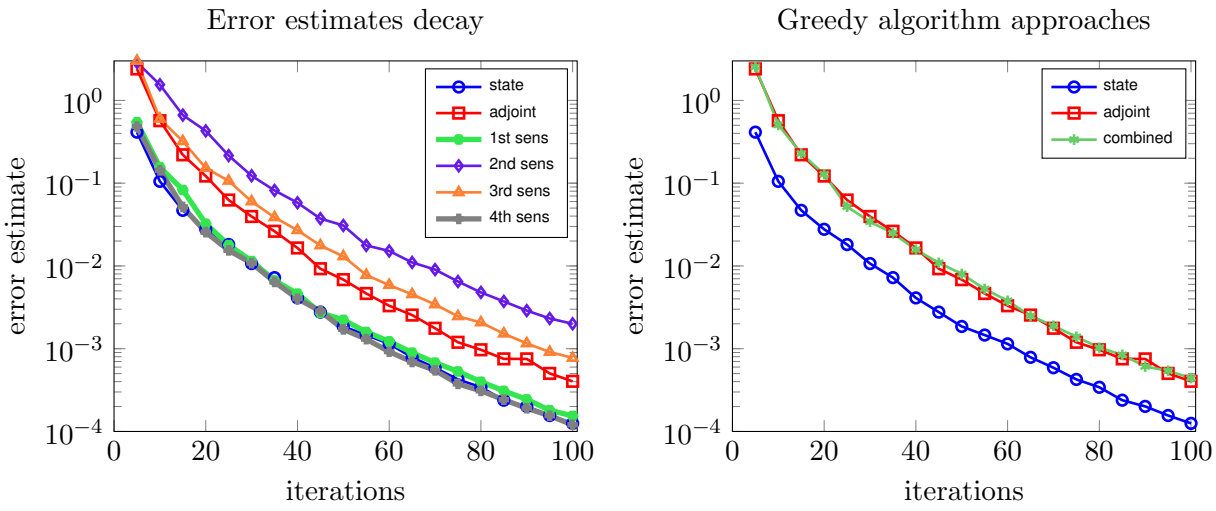

Figure 2. Convergence of the three greedy algorithms presented in Section 4.3.

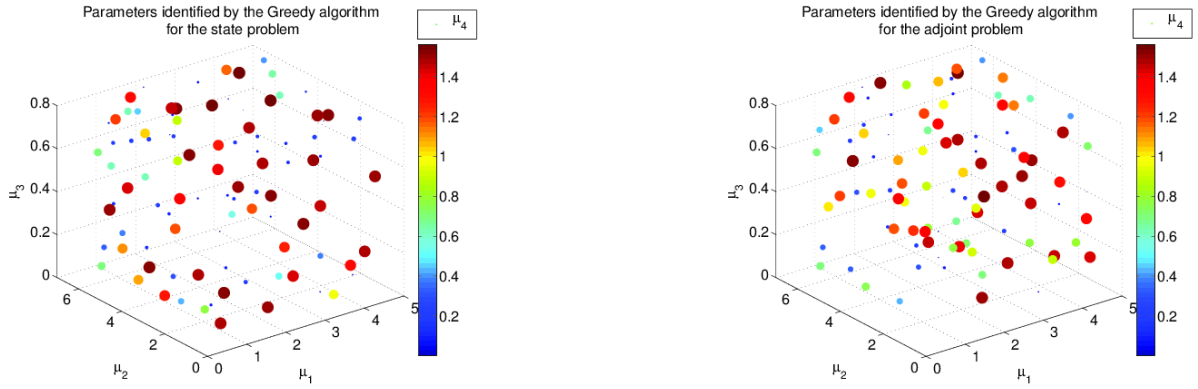

Figure 3. Sampled parameters during the greedy algorithm for state (left) and adjoint (right) problems.

Table 1. CPU time (minutes) for the *offline* stage, for different greedy algorithms.

	$N = 30$	$N = 50$	$N = 70$	$N = 90$	$N = 110$
state+adjoint (Alg. 4.1)	6 m	9.5 m	13.5 m	17.5 m	22 m
state+sensitivities (Alg. 4.3)	8 m	13 m	19 m	25 m	32 m

6.1.2. *Online stage*

We now compare the (reduced) descent methods introduced in Sect. 4.2 – namely, projected gradient, quasi-Newton and Newton methods – prescribing a stopping criterium based on the gradient of the cost functional $\|\nabla_{\boldsymbol{\mu}} J_n\|_{\mathbb{R}^d}$. In a first test case we start from $\boldsymbol{\mu}^{(0)} = (1, 1, 0.01, \frac{\pi}{2})$ and we apply the gradient algorithm by considering either the Armijio rule or the line-search method for choosing the step size. The method converges to the optimal value $\boldsymbol{\mu}_{target}$, although it requires a large number of iterations (and subiterations for the step size criterium); state and adjoint solutions are reported in Fig. 4.

Provided that the cost functional is non-convex with respect to $\boldsymbol{\mu}$, the reduced quasi-Newton method converges only if the starting value $\boldsymbol{\mu}^{(0)}$ is sufficiently close to the optimal value. As a consequence, we exploit the gradient algorithm (globally convergent) to generate a suitable starting point for the quasi-Newton method. In this case, we run the gradient method until it satisfies the stopping criterium with tolerance $tol = 10^{-2}$, then we turn to the quasi-Newton method. This combination allows us to achieve very high accuracy with a limited number of iterations (e.g. 18 iterations of gradient method with line-search rule plus 7 of Newton method in order to reach a tolerance of 10^{-9} in the stopping criterium). A stagnation effect on the cost functional, yielding a convergence of the reduced descent method to an optimal value $\hat{\boldsymbol{\mu}}_n \nrightarrow \boldsymbol{\mu}_{target}$, is observed in the case of a poor RB approximation, see Fig. 5, for both

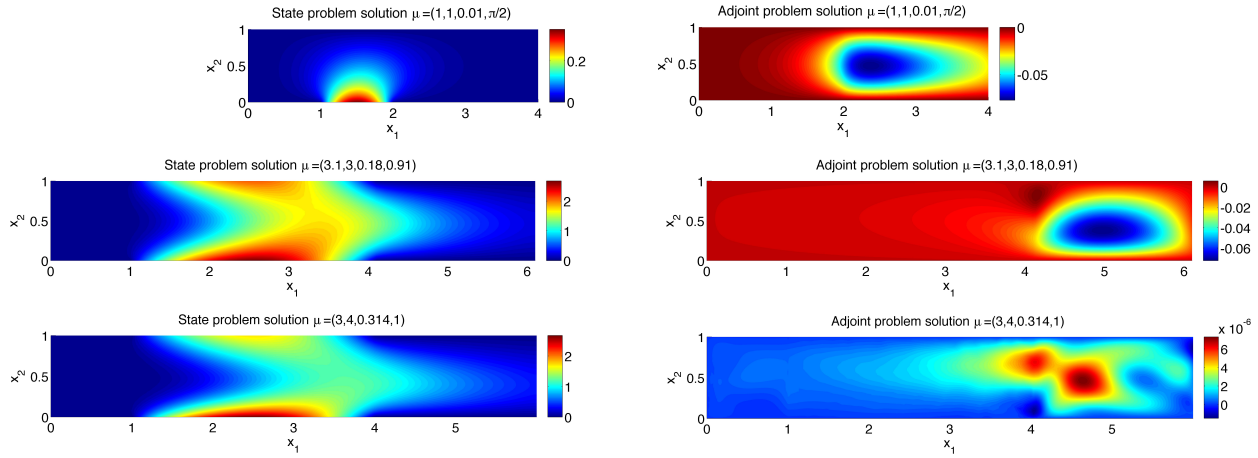

Figure 4. RB state and adjoint solutions for $\boldsymbol{\mu} = \boldsymbol{\mu}^{(0)}$ (top), $\boldsymbol{\mu} = \boldsymbol{\mu}^{(3)} = (3.1, 3, 0.18, 0.91)$ (middle), $\boldsymbol{\mu} = \hat{\boldsymbol{\mu}}_n$ (bottom).

Newton and quasi-Newton methods; a similar conclusion is found for the gradient method.

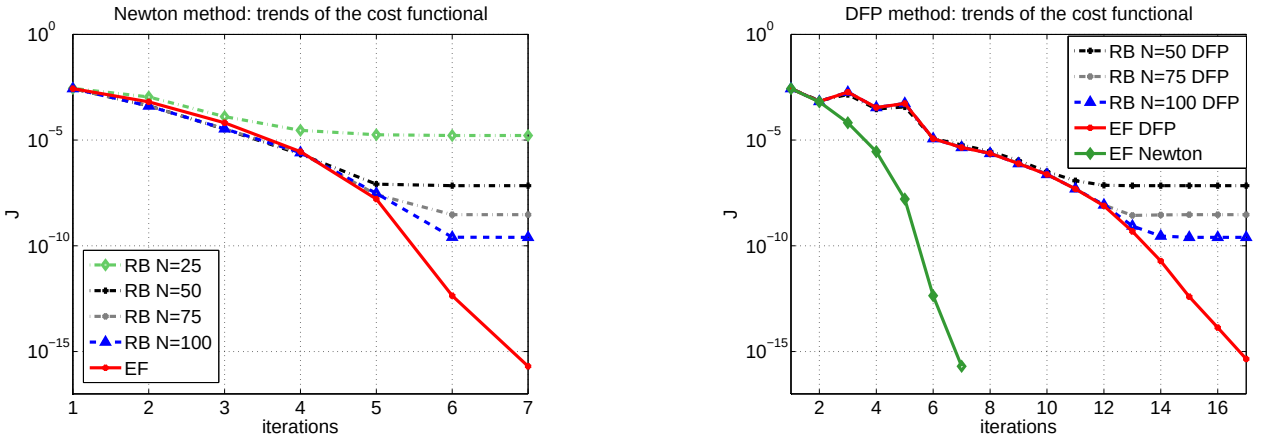

Figure 5. Cost functional values at each iteration of Newton (left) and quasi-Newton (right) methods for different RB dimensions N and comparison with the high-fidelity FE approximation.

Hence, already for RB subspaces of relatively small dimension ($N = 75, 100$), a remarkable accuracy is reached. Concerning the CPU time required to perform optimization, we pursue a computational speedup ranging from 17 in the Newton case to 93 in the gradient case. The smallest number of iterations required to reach convergence is obtained in the Newton case (see Table 2).

Table 2. Number of iterations and computational times of the Gradient method with Armijio rule and inexact line-search in $(10^{-2}, 50)$ with 500 samples, of quasi-Newton and Newton methods ($N = 100$ RB functions). $CPUtime/it_{RB}$ and $CPUtime/it_{FE}$ denote the CPU time required to perform *online* a single step of the optimization procedure when relying on the RB or the FE approximation, respectively.

	$\#it_{RB}$	$CPUtime/it_{RB}$	$CPUtime/it_{FE}$
Gradient (Armijio)	2502	0.0104 s	0.9327 s
Gradient (line search)	173	1.926 s	59.027 s
Gradient (line search) + quasi-Newton	$18 + 17$	0.0088 s	0.1249 s
Gradient (line search) + Newton	$18 + 7$	0.0235 s	0.4047 s

The best option concerning computational efficiency is the quasi-Newton method. For the case at hand, using the gradient method to generate a suitable starting point $\tilde{\boldsymbol{\mu}}_0$, the quasi-Newton (DFP) method converges in 17 iterations to the sub-optimal value $\hat{\boldsymbol{\mu}}_n = (2.99996, 4.00002, 0.31416, 0.99996)$, with cost functional $J_n(\hat{\boldsymbol{\mu}}_n) = 2.51\ 10^{-10}$. In particular, we initialize the surrogate of the Hessian matrix $\mathbb{H}_J(\boldsymbol{\mu})$ with a diagonal matrix of elements equal to the step size identified by the inexact line search (as in

a step of the gradient method). Starting form the same initial guess $\tilde{\boldsymbol{\mu}}_0$, the Newton method converges in 7 iterations to $\hat{\boldsymbol{\mu}}_n = (2.99996, 4.00003, 0.314164, 0.99996)$, with cost functional $J_n(\hat{\boldsymbol{\mu}}_n) = 2.51\ 10^{-10}$. We remark that the accuracy of the reduced-order model (in terms of the number n of basis functions) has a relevant role in achieving the minimum value of the cost functional: the larger n, the smaller $J_n(\hat{\boldsymbol{\mu}}_n)$, see Fig. 5 – recall that $\hat{\boldsymbol{\mu}} = \boldsymbol{\mu}_{target}$. In addition to its better efficiency with respect to the sensitivity-based approach, the adjoint-based method yields inexpensive a posteriori error estimates for the cost functional and its gradient. In this case, the effectivities

$$\eta_J(\boldsymbol{\mu}) = \frac{\Delta_n^J(\boldsymbol{\mu})}{|J_h(\boldsymbol{\mu}) - J_n(\boldsymbol{\mu})|}, \qquad \eta_{\nabla J}(\boldsymbol{\mu}) = \frac{\Delta_n^{\nabla J}(\boldsymbol{\mu})}{\|\nabla_{\boldsymbol{\mu}} J_h(\boldsymbol{\mu}) - \nabla_{\boldsymbol{\mu}} J_n(\boldsymbol{\mu})\|_{\mathbb{R}^d}}$$

for J and ∇J, respectively, are indeed very close to 1 – that is, the proposed error estimate show to be very tight for the case at hand, see Fig. 6. This is in our opinion a remarkable result, since error estimates usually show large effectivities in the case of optimal control problems, see e.g. [4,5].

	η_J	$\eta_{\nabla J}$
$N = 30$	2.0716	4.3478
$N = 65$	1.2286	4.5187
$N = 90$	1.1121	4.1614

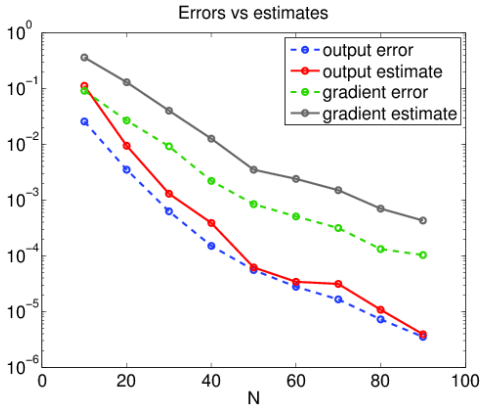

Figure 6. A posteriori error estimates for the cost functional and its gradient: effectivities (left) and behavior with respect to the RB dimension N, average on a sample $\Xi_{test} \subset \mathcal{P}$ of dimension 100 (right).

Finally, to assess the accuracy of the proposed framework, we evaluate the error $\|\hat{\boldsymbol{\mu}}_j - \hat{\boldsymbol{\mu}}_n\|$ between the high-fidelity and the reduced-order solution of the optimization problems. We also verify from a computational standpoint the result of Theorem 5.1, focusing on the dependence of the error estimate (36) on the RB dimension n and the tolerance ε_{opt}^{tol} of the stopping criterium. These results confirm that achieving a very good approximation of the optimality conditions in a neighborhood of the optimal solution is essential to guarantee a good approximation of the optimal parameters. In fact, the estimate is only certified for a number of basis functions greater than 90, which decreases noticeably the error $\|\nabla_{\boldsymbol{\mu}} J_n(\boldsymbol{\mu}) - \nabla_{\boldsymbol{\mu}} J_h(\boldsymbol{\mu})\|_{\mathbb{R}^d}$ (and so ϵ). On the other hand for tolerances smaller than 10^{-5} and 100 basis the estimate is always verified.

6.2. *NACA airfoil shape design*

We now turn to the optimal design of NACA airfoils. Parametrizing the airfoil shape enables to cast the problem into the PDE-constrained parametric optimization framework presented in this paper. In our case we deal with $d = 3$ parameters, namely

- $\mu_1 \in [0.04, 0.24]$ the maximum thickness of the airfoil;
- $\mu_2 \in [0, 0.012]$ the curvature of the wing profile;
- $\mu_3 \in [-0.45\pi, 0.45\pi]$ the angle of incidence of the flow w.r.t. the chord of the airfoil.

We consider a set of affine maps (naturally induced by the selected parameters) defined over a domain decomposition[f] in order to fulfill the affine parametric dependence property (4), as shown e.g. in [40].

[f] In this respect, the domain is partitioned into several (standard, elliptical or curvy) triangles. A piecewise affine mapping based on this domain decomposition is then built. For the sake of length, here we do not report the procedure followed to construct these maps; detailed steps, tailored to the case of two-dimensional NACA airfoil profiles, can be found in [46].

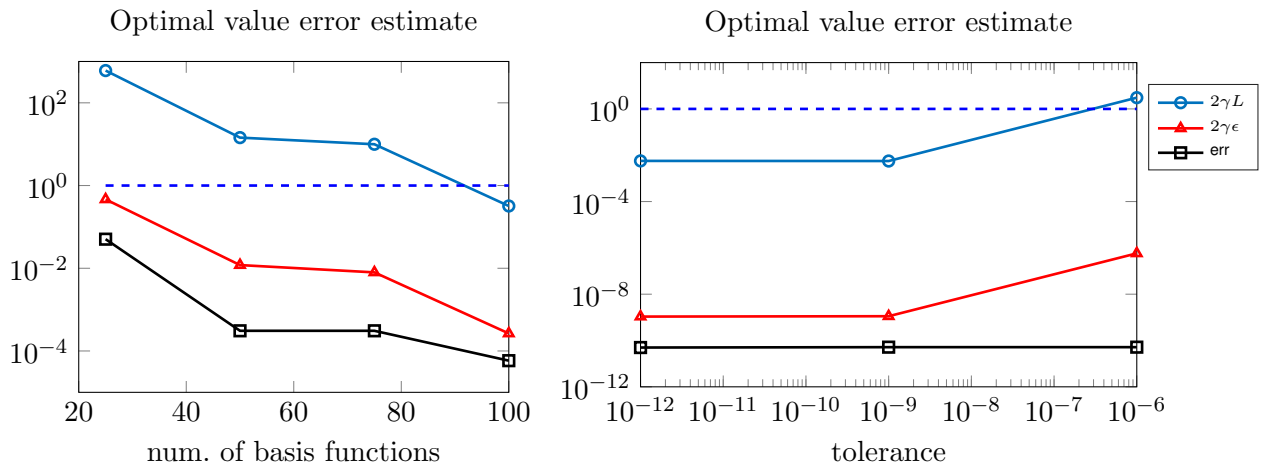

Figure 7. A posteriori error estimates for the optimal parameters (Newton method started with line search gradient iterations) varying the number of basis functions N at fixed tolerance $\epsilon_J = 10^{-6}$ of the stopping criterium for the optimization (left) and varying ϵ_J at fixed $N = 100$ (right).

This yields $Q_a = 184$ and $Q_f = 188$ terms in expression (4), respectively. Other options to deal with more general nonaffine[g] maps and parametrization – such as (discrete) empirical interpolation – can also be used, see e.g. [24,26,47]. We describe the flow around the airfoil through a potential model, leading to the following state problem for the velocity potential: find $\phi \in X$ such that

$$
\begin{cases}
-\Delta\phi = 0 & \text{in } \tilde{\Omega}(\mu_1, \mu_2) \\
\phi = \phi_{ref}(\mu_3) & \text{on } \tilde{\Gamma}_{out} \\
\dfrac{\partial \phi}{\partial n} = \mathbf{u}_{in}(\mu_3) \cdot \mathbf{n} & \text{on } \tilde{\Gamma}_{in} \\
\dfrac{\partial \phi}{\partial n} = 0 & \text{on } \tilde{\Gamma}_{wing}(\mu_1, \mu_2).
\end{cases} \tag{39}
$$

The velocity-pressure formulation follows by the identity $\mathbf{u} = -\nabla\phi$ and the Bernoulli equation. Following [48, Chapter 2], we aim at reconstructing the airfoil shape corresponding to a given target velocity field in the rear $\tilde{\Omega}_{obs} \subset \Omega$ of the airfoil, that is, to approximate

$$
\hat{\boldsymbol{\mu}}_h = \arg\min_{\boldsymbol{\mu}\in\mathcal{P}} J_h(\boldsymbol{\mu}), \quad J_h(\boldsymbol{\mu}) = \frac{1}{2}\int_{\tilde{\Omega}_{obs}} |\nabla(\phi_h(\boldsymbol{\mu}) - z_d)|^2 d\Omega. \tag{40}
$$

Here the target is $z_d = \phi_h(\boldsymbol{\mu}_{target})$ with $\boldsymbol{\mu}_{target} = (0.15, 0.006, \frac{\pi}{6})$.

Remark 6.1. This test case has been chosen to show how the proposed framework can also deal with more involved geometrical parametrizations. Some relevant physical elements are missing, such as the Kutta condition applied at the trailing edge of the profile; see, e.g., [49] for a detailed description of how to construct a reduced order model in this case. With slight modifications, a thermal flow shape optimization problem around the airfoil, similar to the one addressed in [25,50], can also be obtained.

6.2.1. *Offline stage*

The approximation of the problem (39)–(40), mapped onto the fixed reference domain Ω, is firstly obtained through the Galerkin FE method with linear finite elements, resulting in a high-fidelity approximation of dimension $N_h = 10886$. Then, we exploit the greedy Algorithms 4.1 and 4.3 for constructing the

[g] Indeed, affine parameter dependence is mandatory to ensure the offline-online splitting. In the case of *nonaffine* problems, hyper-reduction techniques such as the empirical interpolation method (EIM) or the discrete empirical interpolation method (DEIM) are employed before assembling the arrays of the RB problem. Once this *pre-processing* step has been performed, the construction of the RB approximation follows the same procedure described in the paper. Here we have decided to focus on affine problems to better highlight computational difficulties entailed by optimization; however, the proposed techniques can be applied in a straightforward way to nonaffine problems, too.

RB spaces for state and adjoint (resp., sensitivity) problems. Also in this case, the adjoint-based method seems to be more effective in terms of accuracy and efficiency, see Fig. 8 and Table 3; the retained snapshots are reported in Fig. 9.

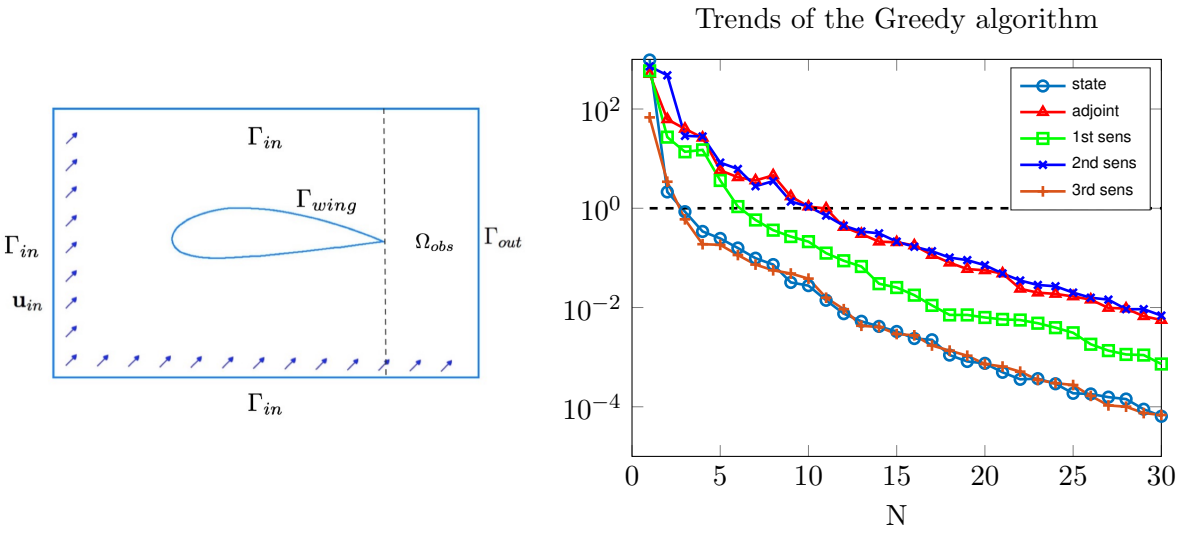

Figure 8. Schematic representation of the domain Ω (left) and convergence of greedy Algorithm 1 (resp. 3) for state and adjoint (resp. sensitivity) problems (right).

Table 3. CPU time for the *offline* stage, for different greedy algorithms.

Basis computation	$N = 10$	$N = 20$	$N = 30$
state+adjoint (Alg. 4.1)	10 m	20 m	31 m
state+sensitivities (Alg. 4.3)	24 m	47 m	72 m

As expected, the offline computational cost are higher with respect to the previous case, because of the larger dimension N_h of the FE space and the larger number Q_a, Q_f of terms in the affine expansion. Indeed, this yields a higher complexity in the $\boldsymbol{\mu}$-dependence of the PDE solutions and additional costs in the assembling of $\boldsymbol{\mu}$-independent arrays.

6.2.2. *Online stage*

Starting from the initial guess $\boldsymbol{\mu}^{(0)} = (0.08, 0.012, -\frac{\pi}{4})$, we compare the results obtained with the reduced and the high-fidelity optimization framework (see Algorithm 4.4), testing different options concerning the descent directions. For the case at hand, the Newton method converges considering $\boldsymbol{\mu}_n^{(0)} = (0.08, 0.012, -\frac{\pi}{4})$ as initial guess. The iterations generated by the high-fidelity and the reduced Newton method (varying the number of basis functions) are displayed in Fig. 10, top and Fig. 11, left.

Clearly, the results obtained with the reduced optimization algorithm get closer and closer to the high-fidelity solution as the number of RB functions increases. The RB approximation of both state and adjoint problems are reported in Fig. 12 for different parameter values (initial guess, second iteration of the Newton method and optimal parameter value); the corresponding velocity and pressure fields are reported in Fig. 13.

On the other hand, the quasi-Newton method (with $H^{(0)}$ equal to the identity matrix) requires about the three times the number of iterations to converge with respec to the Newton method, yet entailing a remarkably lower computational effort (both during the *offline* and *online* phase). The iterations generated by the high-fidelity and the reduced quasi-Newton method are displayed in Fig. 10, bottom and Fig. 11, right.

In order to control the reduction error at each step of the minimization procedure, we can rely on the proposed error estimates. In particular, we compute the effectivities of the error estimator for the cost

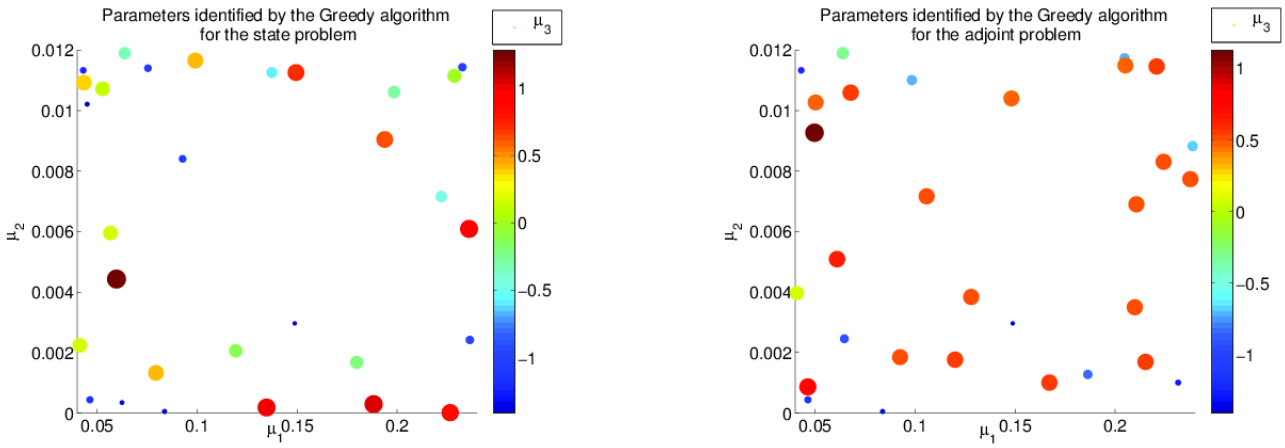

Figure 9. Sampled parameters during the greedy algorithm for state (left) and adjoint (right) problems.

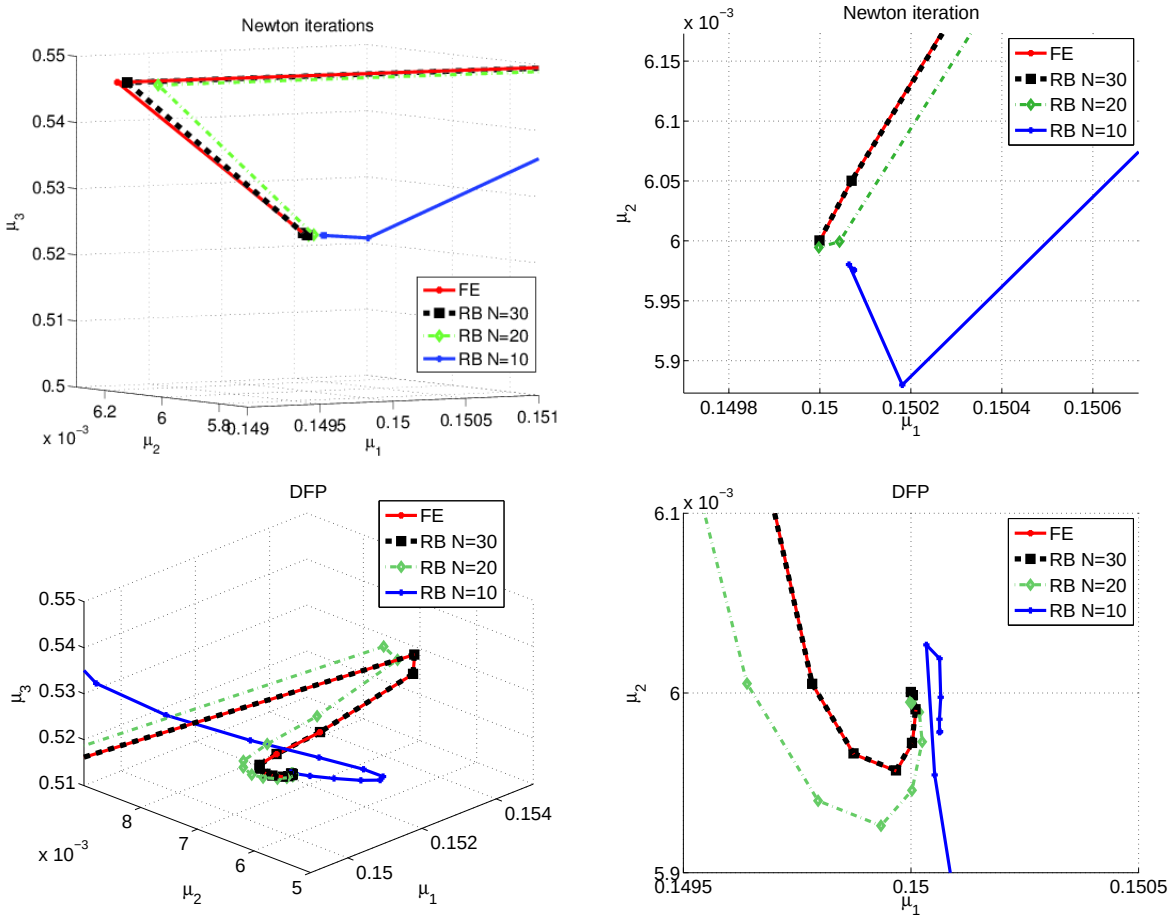

Figure 10. Iterations of Newton method (top) and quasi-Newton method (bottom) in the parameter space.

functional and its gradient (see Fig. 14). As in the previous example, the goal-oriented analysis provides a tight error estimate for the cost functional J, and a reliable (but less tight) error estimate in the case of the gradient ∇J. Moreover, we can assess the influence of reduction errors on the optimal solution thanks to the result of Theorem 5.1. We report in Fig. 15 the error estimate (36) for different RB dimensions n and tolerances ε_{opt}^{tol} of the stopping criterium.

By considering a RB dimension greater than 9 and a tolerance $\varepsilon_{opt}^{tol} < 5 \cdot 10^{-3}$, the hypothesis of Theorem 5.1 are verified. Hence, (36) provides a reliable estimate of the error $\|\hat{\boldsymbol{\mu}}_h - \hat{\boldsymbol{\mu}}_n\|_{\mathbb{R}^p}$ on the

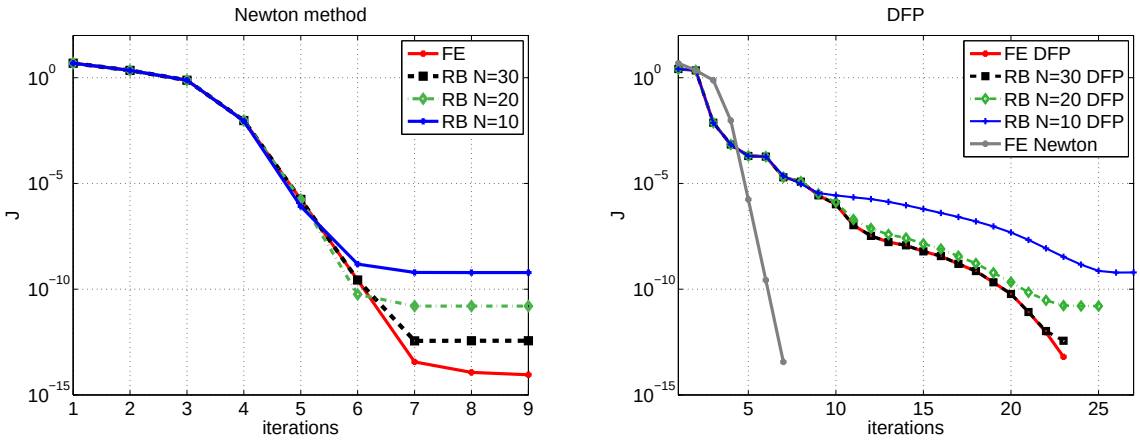

Figure 11. Trend of the cost functional for Newton (left) and quasi-Newton method (right).

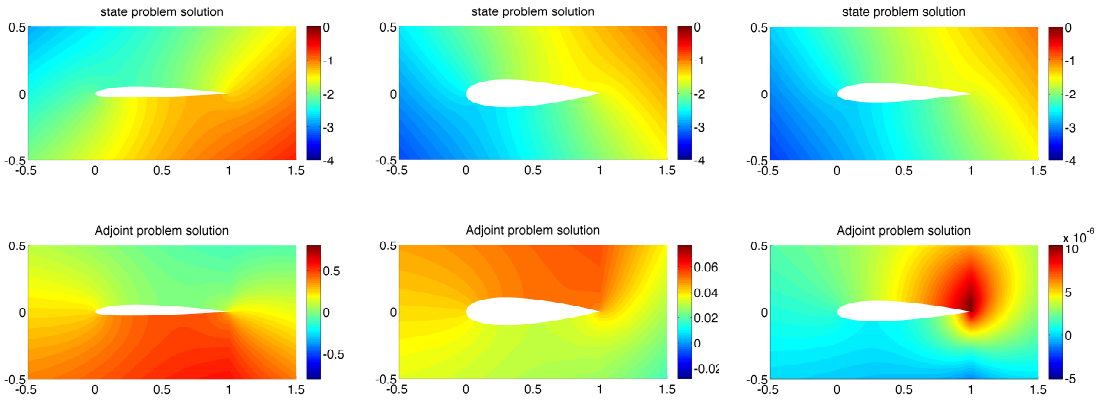

Figure 12. Solutions of the state and adjoint problems for $\boldsymbol{\mu}_n^{(0)} = (0.08, 0.012, -\frac{\pi}{4})$ (left), $\boldsymbol{\mu}_n^{(2)} = (0.2029, 0, 0.5759)$ (center) and $\hat{\boldsymbol{\mu}}_n = (0.1501, 0.006, 0.5236)$ (right).

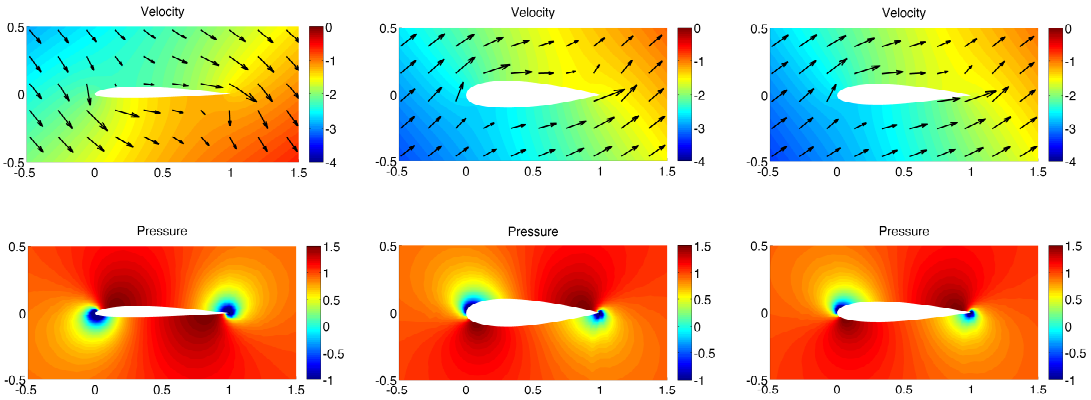

Figure 13. Velocity and pressure fields for $\boldsymbol{\mu}_n^{(0)} = (0.08, 0.012, -\frac{\pi}{4})$ (left), $\boldsymbol{\mu}_n^{(2)} = (0.2029, 0, 0.5759)$ (center) and $\hat{\boldsymbol{\mu}}_n = (0.1501, 0.006, 0.5236)$ (right).

optimal parameter values.

Finally, we report some details concerning the computational costs, by considering as starting point $\boldsymbol{\mu}_n^{(0)} = (0.22, 0.01, 0.4\pi)$ with a tolerance $\varepsilon_{opt}^{tol} = 10^{-10}$ for the reduced optimization procedure. As expected, the gradient method requires several iterations to satisfy the stopping criterium – this is due to the elongated shape of the level sets of the cost functional, see Fig. 10. The smallest number of iterations required to reach convergence is obtained in the Newton case (see Table 4).

Table 4. Number of iterations and CPU times of the gradient method with Armijio rule and inexact line-search in $(10^{-2}, 50)$ with 500 samples, of quasi-Newton and Newton methods ($N = 30$ RB functions). $CPUtime/it_{RB}$ and $CPUtime/it_{FE}$ denote the CPU time required to perform *online* a single step of the optimization procedure when relying on the RB or the FE approximation, respectively.

	$\#it_{RB}$	$CPUtime/it_{RB}$	$CPUtime/it_{FE}$
Gradient (Armijio)	1699	0.0788 s	1.5001 s
Gradient (l-s)	626	10.58 s	191.5 s
Gradient (l-s) + quasi-Newton	$12 + 37$	0.0385 s	0.7951 s
Gradient (l-s) +Newton	$12 + 8$	0.0917 s	1.4944 s

For the sake of comparison, we report in Table 5 the total computational cost entailed by the reduced optimization, including also the offline construction of the RB spaces, see Table 3 for the CPU times concerning this latter operation. We consider $N = 30$ RB functions and *(i)* the greedy Algorithm 1 for the gradient and the quasi-Newton methods, *(ii)* the greedy Algorithm 3 including the reduction of the sensitivity equations for the Newton method, respectively.

Performing the reduced optimization during the online stage provides a speedup of about 20 for any chosen method. We get a computational speedup also including both offline and online costs, except for

	η_J	$\eta_{\nabla J}$
$N = 10$	28.4091	1000
$N = 20$	2.2999	454.5455
$N = 30$	1.9201	416.6667

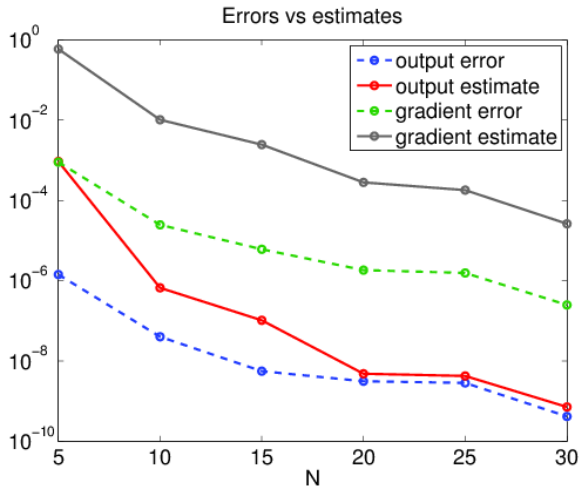

Figure 14. A posteriori error estimates for the cost functional and its gradient: effectivities (left) and behavior with respect to the RB dimension N, average on a sample $\Xi_{test} \subset \mathcal{P}$ of dimension 100 (right).

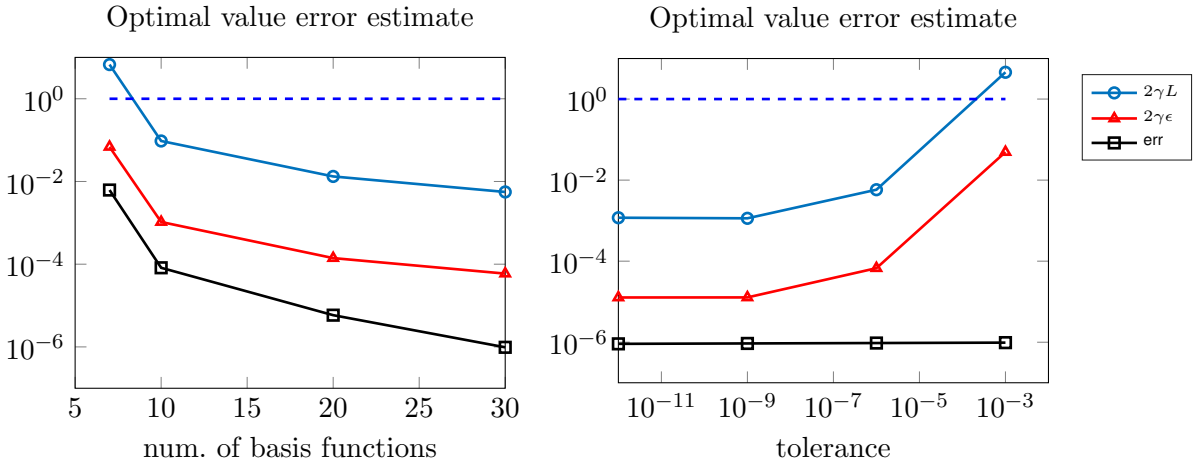

Figure 15. A posteriori error estimates for the optimal parameters (Newton method started with line search gradient iterations) varying the number of basis functions (left) and the tolerance of the stopping criterium (right).

Table 5. Overall computational times for the RB (offline+online) and the high-fidelity FE optimization. Offline and online time refer to the construction of the RB approximation and to the (reduced) optimization procedure, respectively.

	RB offline	RB online	FE
Gradient (Armijio)	31 m	2.21 m	42.47 m
Gradient (l-s)	31 m	110.38 m	1998 m
Gradient (l-s) + quasi-Newton	31 m	2.14 m	38.69 m
Gradient (l-s) +Newton	72 m	2.13 m	38.39 m

the Newton method, which requires however the construction of $d+1 > 2$ RB spaces (state + d sensitivity equations). In the case of a single solution of the optimization problem, we save about 20%, 90% and 15% of the CPU time in the case of the gradient method with the Armijio rule, with line search and of the quasi-Newton method, respectively. The gain is even larger if more than one optimization problem has to be solved online, for instance by varying the target function z_d: in this case the offline stage must not be run again, and the optimization just requires a very fast online stage (order of 2 minutes). Last but not least, a possible restarting of the optimization algorithm, whenever required, can be performed inexpensively.

7. Conclusions

In this work we have proposed a certified reduced basis method for the efficient solution of PDE-constrained parametric optimization problems. We have compared *(i)* a sensitivity-based and *(ii)* an adjoint-based approach, relying in both cases on the reduced basis method to speedup the PDE solution at each step of a descent optimization algorithm. We have also provided a posteriori error estimates for the cost functional, its gradient and the optimal solution in order to control the accuracy of both descent directions evaluated through the RB framework and optimal solutions resulting from the application of the proposed reduced framework. Numerical test cases assess the validity of the theoretical results and the efficiency of the proposed reduced-order methodology. Two cases have been considered, dealing with *(i)* the optimal control of thermal flows and *(ii)* the optimal design of airfoil profiles in a simplified potential flow. In both cases, the adjoint-based approach, together with a quasi-Newton method for numerical optimization, provide the best tradeoff in terms of accuracy and computational efficiency.

Acknowledgements

We are grateful to Prof. Sandro Salsa (Politecnico di Milano) for the scientific discussions and the support provided, and to Dr. Luca Dedè (Politecnico di Milano) for his useful advices and feedbacks.

Appendix

7.1. *Proof of Proposition 3.1*

Thanks to (1)-(2), the Lax-Milgram lemma, and assumption 2., the map $\boldsymbol{\mu} \to u(\boldsymbol{\mu})$ defines a bounded injective operator; moreover,

$$\|u(\boldsymbol{\mu}) - u(\bar{\boldsymbol{\mu}})\|_X \leq \frac{1}{\alpha(\boldsymbol{\mu})} \left(\sum_{q=1}^{Q_f} M_f^q \Lambda_q^f + \frac{M_f(\bar{\boldsymbol{\mu}})}{\alpha(\bar{\boldsymbol{\mu}})} \sum_{q=1}^{Q_a} M_a^q \Lambda_q^a \right) \|\boldsymbol{\mu} - \bar{\boldsymbol{\mu}}\|_{\mathbb{R}^d}. \tag{41}$$

Assumption 3. is verified since J is given by the composition of a continuous function and a semi-continuous one. The existence of a minimizer then follows thanks to the Weierstrass theorem. □

7.2. *Proof of Proposition 3.2*

In order to apply the implicit function theorem, we rewrite the state problem appearing in (6) by isolating a $\boldsymbol{\mu}$-independent injective[b] operator Π, as: find $u \in X$ such that

$$\Pi u + \sum_{q=2}^{Q_a} \tilde{\Theta}_q^a(\boldsymbol{\mu}) A_q u - \sum_{q=1}^{Q_f} \tilde{\Theta}_q^f(\boldsymbol{\mu}) F_q = 0 \qquad \text{in } X^*.$$

Then, we define the operator

$$\Phi : X \times \mathcal{P} \to X^* : (u, \boldsymbol{\mu}) \to \sum_{q=1}^{Q_f} \tilde{\Theta}_q^f(\boldsymbol{\mu}) F_q - \sum_{q=2}^{Q_a} \tilde{\Theta}_q^a(\boldsymbol{\mu}) A_q u.$$

Thanks to the continuity of the forms $a^q(\cdot,\cdot)$ and $f_q(\cdot)$ and since the functions Θ_q^a, $q = 1, \ldots, Q_a$ and Θ_q^f, $q = 1, \ldots, Q_f$ are of class $C^1(\mathcal{P})$, Φ is Fréchet differentiable. For any $\boldsymbol{\mu}$, let us denote by $\Pi^{-1} : X^* \to X$ the inverse of the injective operator yielding the unique solution of $\Pi y = v$ in X^*. We can formulate the state problem as

$$F(u, \boldsymbol{\mu}) = u - \Pi^{-1}(\Phi(u, \boldsymbol{\mu})) = 0; \tag{42}$$

Π^{-1} is continuously differentiable (since it is linear) and, for a reference value $\bar{\boldsymbol{\mu}}$ (yielding $\bar{u} = u(\bar{\boldsymbol{\mu}})$), we obtain, by applying the chain rule to F,

$$F_u(\bar{u}, \bar{\boldsymbol{\mu}})v = v - \Pi^{-1}(\Phi_u(\bar{u}, \bar{\boldsymbol{\mu}})v) \qquad \forall v \in X.$$

Here $F_u(\bar{u}, \bar{\boldsymbol{\mu}})$ is an isomorphism in X, since the problem

$$v - \Pi^{-1}(\sum_{q=1}^{Q_a} \Theta_q^a(\boldsymbol{\mu}) A_q v) = w \tag{43}$$

has a unique solution $\forall w \in X$. Thanks to the implicit function theorem, (42) defines a map $\boldsymbol{\mu} \mapsto u(\boldsymbol{\mu})$, with $u \in C^1(\mathcal{P})$ in a neighborhood of $\bar{\boldsymbol{\mu}}$. □

References

1. A. Borzì and V. Schulz, *Computational Optimization of Systems Governed by Partial Differential Equations*. SIAM, 2011.
2. M. Hinze, R. Pinnau, M. Ulbrich, and S. Ulbrich, *Optimization with PDE Constraints*. Springer, 2009.
3. A. Quarteroni, G. Rozza, and A. Quaini, Reduced basis methods for optimal control of advection-diffusion problem, in *Advances in Numerical Mathematics, W. Fitzgibbon, R. Hoppe, J. Periaux, O. Pironneau, and Y. Vassilevski, Editors*, pp. 193–216, 2007.
4. L. Dedè, Reduced basis method and a posteriori error estimation for parametrized linear-quadratic optimal control problems, *SIAM Journal on Scientific Computing*, vol. 32, no. 2, pp. 997–1019, 2010.
5. L. Dedè, Reduced basis method and error estimation for parametrized optimal control problems with control constraints, *Journal of Scientific Computing*, vol. 50, no. 2, pp. 287–305, 2012.
6. T. Tonn, K. Urban, and S. Volkwein, Comparison of the reduced basis and pod a posteriori error estimators for an elliptic linear-quadratic optimal control problem, *Mathematical and Computer Modelling of Dynamical Systems*, vol. 17, no. 4, pp. 355–369, 2011.

[b] If one of the bilinear forms $a_q(\cdot,\cdot)$ is coercive, identifying Π is straightforward thanks to the Riesz representation theorem, by taking $\tilde{\Theta}_q^a(\boldsymbol{\mu}) = \Theta_q^a(\boldsymbol{\mu})/\Theta_1^a(\boldsymbol{\mu})$, $q = 2, \ldots, Q_a$, and $\tilde{\Theta}_q^f(\boldsymbol{\mu}) = \Theta_q^f(\boldsymbol{\mu})/\Theta_1^a(\boldsymbol{\mu})$, $q = 1, \ldots, Q_f$.

7. M. A. Dihlmann and B. Haasdonk, Certified PDE-constrained parameter optimization using reduced basis surrogate models for evolution problems, *Computational Optimization and Applications*, vol. 60, no. 3, pp. 753–787, 2015.
8. M. Dihlmann and B. Haasdonk, Certified nonlinear parameter optimization with reduced basis surrogate models, *Proceedings in Applied Mathematics & Mechanics*, vol. 13, no. 1, pp. 3–6, 2013.
9. Y. Zhang, L. Feng, S. Li, and P. Benner, Accelerating PDE constrained optimization by the reduced basis method: application to batch chromatography, *International Journal for Numerical Methods in Engineering*, vol. 104, no. 11, pp. 983–1007, 2015.
10. K. Kunisch and S. Volkwein, Proper orthogonal decomposition for optimality systems, *ESAIM: Mathematical Modelling and Numerical Analysis*, vol. 42, no. 1, pp. 1–23, 2008.
11. M. Kahlbacher and S. Volkwein, Galerkin proper orthogonal decomposition methods for parameter dependent elliptic systems, *Disc. Math.: Diff. Incl., Control and Optim.*, vol. 27, pp. 95–117, 2007.
12. E. W. Sachs and S. Volkwein, Pod-Galerkin approximations in pde-constrained optimization, *GAMM-Mitteilungen*, vol. 33, no. 2, pp. 194–208, 2010.
13. M. Kahlbacher and S. Volkwein, POD a-posteriori error based inexact SQP method for bilinear elliptic optimal control problems, *ESAIM: Mathematical Modelling and Numerical Analysis*, vol. 46, no. 02, pp. 491–511, 2012.
14. O. Lass, *Reduced Order Modeling and Parameter Identification for Coupled Nonlinear PDE Systems*. PhD thesis, University of Konstanz, 2014.
15. D. Amsallem, M. J. Zahr, Y. Choi, and C. Farhat, Design optimization using hyper-reduced order models, *Struct. Multidisc. Optim.*, 2014.
16. M. Gubisch and S. Volkwein, Pod a-posteriori error analysis for optimal control problems with mixed control-state constraints, *Computational Optimization and Applications*, vol. 58, no. 3, pp. 619–644, 2014.
17. M. Gubisch and S. Volkwein, Proper orthogonal decomposition for linear-quadratic optimal control, in *Model Reduction and Approximation: Theory and Algorithms* (P. Benner, A. Cohen, M. Ohlberger, and K. Willcox, eds.), pp. 5–66, SIAM, 2017.
18. F. Negri, G. Rozza, A. Manzoni, and A. Quarteroni, Reduced basis method for parametrized elliptic optimal control problems, *SIAM Journal on Scientific Computing*, vol. 35, no. 5, pp. A2316–A2340, 2013.
19. F. Negri, A. Manzoni, and G. Rozza, Reduced basis approximation of parametrized optimal flow control problems for the Stokes equations, *Computers & Mathematics with Applications*, vol. 69, no. 4, pp. 319–336, 2015.
20. M. Kärcher and M. Grepl, A certified reduced basis method for parametrized elliptic optimal control problems, *ESAIM: Control, Optimisation and Calculus of Variations*, vol. 20, no. 2, pp. 416–441, 2014.
21. M. Kärcher, Z. Tokoutsi, M. Grepl, and K. Veroy, Certified reduced basis methods for parametrized elliptic optimal control problems with distributed controls, *Journal of Scientific Computing*, vol. 75, no. 1, pp. 276–307, 2018.
22. P. Benner, E. Sachs, and S. Volkwein, Model order reduction for PDE constrained optimization, in *Trends in PDE Constrained Optimization* (G. Leugering, P. Benner, S. Engell, A. Griewank, H. Harbrecht, M. Hinze, R. Rannacher, and S. Ulbrich, eds.), pp. 303–326, Springer International Publishing, 2014.
23. A. Borzì and G. von Winckel, A pod framework to determine robust controls in pde optimization, *Computing and Visualization in Science*, vol. 14, no. 3, pp. 91–103, 2011.
24. A. Manzoni, A. Quarteroni, and G. Rozza, Shape optimization for viscous flows by reduced basis methods and free-form deformation, *International Journal for Numerical Methods in Fluids*, vol. 70, no. 5, pp. 646–670, 2012.
25. T. Lassila and G. Rozza, Parametric free-form shape design with pde models and reduced basis method, *Computer Methods in Applied Mechanics and Engineering*, vol. 199, no. 23–24, pp. 1583–

1592, 2010.

26. F. Negri, A. Manzoni, and D. Amsallem, Efficient model reduction of parametrized systems by matrix discrete empirical interpolation, *Journal of Computational Physics*, vol. 303, pp. 431–454, 2015.
27. M. Grepl, N. Nguyen, K. Veroy, A. Patera, and G. Liu, Certified rapid solution of partial differential equations for real-time parameter estimation and optimization, in *Real-time PDE-Constrained Optimization* (L. Biegler, O. Ghattas, M. Heinkenschloss, D. Keyes, and B. Van Bloemen Waanders, eds.), pp. 197–215, SIAM, 2007.
28. M. Bambach, M. Heinkenschloss, and M. Herty, A method for model identification and parameter estimation, *Inverse Problems*, vol. 29, no. 2, 2013.
29. T. Lassila, A. Manzoni, A. Quarteroni, and G. Rozza, A reduced computational and geometrical framework for inverse problems in haemodynamics, *International Journal for Numerical Methods in Biomedical Engineering*, vol. 29, no. 7, pp. 741–776, 2013.
30. C. Lieberman, K. Willcox, and O. Ghattas, Parameter and state model reduction for large-scale statistical inverse problems, *SIAM Journal on Scientific Computing*, vol. 32, no. 5, pp. 2523–2542, 2010.
31. A. Manzoni, S. Pagani, and T. Lassila, Accurate solution of Bayesian inverse uncertainty quantification problems combining reduced basis methods and reduction error models, *SIAM/ASA Journal on Uncertainty Quantification*, vol. 4, no. 1, pp. 380–412, 2016.
32. M. Zahr, K. Carlberg, and D. Kouri, An efficient, globally convergent method for optimization under uncertainty using adaptive model reduction and sparse grids, *arXiv preprint arXiv:1811.00177*, 2018.
33. A. Quarteroni, A. Manzoni, and F. Negri, *Reduced Basis Methods for Partial Differential Equations. An Introduction*. Springer, 2016.
34. E. Zeidler, *Nonlinear Functional Analysis and its Applications*, vol. I: Fixed-Point Theorems. Springer-Verlag, 1985.
35. J. Nocedal and S. J. Wright, *Numerical Optimization*. Springer New York, 2006.
36. E. Arian, M. Fahl, and E. Sachs, Trust-region proper orthogonal decomposition for flow control, tech. rep., Institute for Computer Applications in Science and Engineering, NASA Langley Research Center, Hampton, VA, 2000. Technical report, DTIC Document.
37. Y. Yue and K. Meerbergen, Accelerating pde-constrained optimization by model order reduction with error control, *SIAM Journal on Optimization*, vol. 23, pp. 1344–1370, 2013.
38. M. J. Zahr and C. Farhat, Progressive construction of a parametric reduced-order model for PDE-constrained optimization, *International Journal for Numerical Methods in Engineering*, vol. 102, no. 5, pp. 1111–1135, 2015.
39. C. Kelley, *Iterative Methods for Optimization*. SIAM, 1999.
40. G. Rozza, D. Huynh, and A. Patera, Reduced basis approximation and a posteriori error estimation for affinely parametrized elliptic coercive partial differential equations, *Archives of Computational Methods in Engineering*, vol. 15, pp. 229–275, 2008.
41. A. Manzoni and F. Negri, Heuristic strategies for the approximation of stability factors in quadratically nonlinear parametrized PDEs, *Advances in Computational Mathematics*, vol. 41, no. 5, pp. 1255–1288, 2015.
42. R. Becker and R. Rannacher, An optimal control approach to a posteriori error estimation in finite element methods, *Acta Numerica*, vol. 10, pp. 1–102, 2001.
43. R. Becker, H. Kapp, and R. Rannacher, Adaptive finite element methods for optimal control of partial differential equations: Basic concept, *SIAM Journal on Control and Optimization*, vol. 39, no. 1, pp. 113–132, 2000.
44. F. Brezzi, J. Rappaz, and P. A. Raviart, Finite dimensional approximation of nonlinear problems, *Num. Math.*, vol. 38, no. 1, pp. 1–30, 1982.
45. G. Caloz and J. Rappaz, Numerical analysis for nonlinear and bifurcation problems, in *Handbook of Numerical Analysis, Vol. V* (P. Ciarlet and J. Lions, eds.), pp. 487–637, Elsevier Science B.V., 1997.

46. G. Rozza and A. Manzoni, Model order reduction by geometrical parametrization for shape optimization in computational fluid dynamics, in *Proceedings of the ECCOMAS CFD 2010, V European Conference on Computational Fluid Dynamics*, 2010.

47. H. Antil, M. Heinkenschloss, and D. C. Sorensen, Application of the discrete empirical interpolation method to reduced order modeling of nonlinear and parametric systems, in *Reduced Order Methods for Modeling and Computational Reduction* (A. Quarteroni and G. Rozza, eds.), pp. 101–136, Springer, 2014.

48. B. Mohammadi and O. Pironneau, *Applied Shape Optimization for Fluids*. Oxford University Press, 2001.

49. A. Manzoni, F. Salmoiraghi, and L. Heltai, Reduced basis isogeometric methods (RB-IGA) for the real-time simulation of potential flows about parametrized NACA airfoils, *Computer Methods in Applied Mechanics and Engineering*, vol. 284, pp. 1147 – 1180, 2015.

50. G. Rozza, T. Lassila, and A. Manzoni, Reduced basis approximation for shape optimization in thermal flows with a parametrized polynomial geometric map, in *Spectral and High Order Methods for Partial Differential Equations. Selected papers from the ICOSAHOM '09 conference, June 22-26, Trondheim, Norway* (J. S. Hesthaven and E. Rønquist, eds.), pp. 307–315, Springer, 2011.